Optimal strokes at low Reynolds number: a geometric and numeric study using the Copepod and Purcell swimmers.

P. Bettiol *

Laboratoire de Mathématiques Unité CNRS UMR 6205, Université de Bretagne Occidentale, 6, Avenue Victor Le Gorgeu, 29200 Brest, France

B. Bonnard †

Inria Sophia Antipolis et Institut de Mathématiques de Bourgogne, 9 avenue Savary, 21078 Dijon, France

J. Rouot ‡

Inria Sophia Antipolis, 2004 route des lucioles, F-06902 Sophia Antipolis, France

In this article, we make a comparative geometric and numeric analysis of the optimal strokes at low Reynolds number using two specific rigid links swimmers: the Copepod swimmer, a symmetric swimmer introduced recently[30] and the historical three-link Purcell swimmer[27] where the cost to minimize is the mechanical power dissipated by the fluid viscous drag forces. This leads to a sub-Riemannian problem which can be analyzed in this rich framework. In particular nilpotent approximation can be used to compute strokes with small amplitudes and they can be continued numerically to compute more general strokes. The concept of geometric efficiency corresponding to the ratio between the displacement and the length of the stroke is introduced to analyze the global optimality. The role of both abnormal and normal strokes is described, in particular in the symmetric case, in relation with observed motions of the micro-organisms. Moreover C^1-optimality is studied using the concept of conjugate and focal points, depending upon their respective shapes. In parallel direct and indirect numerical schemes implemented in the `Bocop` (`www.bocop.org`[6]) and `HamPath` (`www.hampath.org`[14]) software allow to perform numerical simulations, crucial to complete the theoretical study and to evaluate the optimal solutions.

Keywords: Low Reynolds number, Copepod swimmer, Purcell swimmer, SR-geometry, periodic optimal control, second order optimality conditions.

AMS Subject Classification: 49K15, 93C10, 70Q05

1. Introduction

Swimming models at low Reynolds numbers applicable to micro-organisms and restricting to rigid links have been introduced in the fifties[27] and assuming that the

*piernicola.bettiol@univ-brest.fr
†bernard.bonnard@u-bourgogne.fr
‡jeremy.rouot@inria.fr

displacement is performed minimizing the mechanical energy dissipated by the drag forces, the optimal strokes can be determined in the framework of SR-geometry. This area has recently produced a lot of useful results in our study, e.g. the concept of nilpotent approximation[3] and explicit computations of the spheres with small radius[8,1] applicable to parameterize and analyze strokes with small amplitudes. Moreover the role of normal and abnormal geodesics[22,11] and smoothness of the minimizers[28], computations of conjugate points in relation with C^1-optimality (for the fixed initial and final points problem) in the normal and abnormal case[8,1] are important issues in our specific problem.
Also the concept of optimal strokes is related to *periodic* optimal control and is connected to the standard problem of finding periodic solutions of Hamiltonian vector fields. This problem was introduced by Poincaré in relation with the N-body problem[25] and well studied by this seminal contributor using continuation and variational methods: existence of one-parameter family of periodic trajectories emanating from an equilibrium point[24], direct methods to compute periodic solutions, in relation with the class of homotopy associated with the topology induced by collisions. All contributions valuable to direct and indirect numerical schemes like in the `Bocop` and `HamPath` software[6,14], and understanding the shape of the optimal strokes, related to the singular configurations of the n-link swimmer.

Altogether the problem boils down to generate multi-parameters family of periodic solutions whose optimality can be analyzed C^1-locally, which corresponds to the notion of weak minimizers, using the concept of conjugate points[8,2], the concept of focal points taking into account non-uniqueness of minimizers[15] or globally with the notion of geometric efficiency, a simplification of the concept of efficiency of a swimmer[30]. More precisely our article will solve the following questions in relation with the swimmer problem.

First of all, considering the problem of fixing a displacement of a given stroke, the necessary optimality conditions related to the notion of conjugate points are applicable to select only simple loop strokes as candidate to optimality (in the normal case)[7]. Such necessary conditions being complemented by sufficient conditions[15] taking into account non-uniqueness of minimizers in our problem in relation with symmetry properties. In particular, it will be a non academic test bed to the conditions mentioned previously. Secondly the problem leads to analyze the following practical problem. Parameterizing by arc-length using the metric defined by the mechanical energy (or any other metric) allows to formulate the problem as a time minimal control problem. Assuming that the distance is achieved by a sequence of n-strokes (n being not fixed) then the concept of geometric efficiency and the analysis of the corresponding optimal problem, allow to find the optimal solution.

Another very interesting question raises by the swimmer problem is the role of abnormal strokes. In particular, in this article using the Copepod swimmer and the concept of efficiency, the triangular abnormal stroke[30] is shown to be non optimal since a better policy is to reproduce twice a smooth stroke, producing the same displacement. Although this policy is not C^0-closed from the abnormal stroke, it

opens a new road to deal with non smooth abnormal geodesics in SR-geometry.

Finally, a contribution of this article is to gather nilpotent approximation in SR-geometry and numeric continuation methods useful in particular for the Purcell swimmer to compute strokes of larger amplitudes starting from strokes with small amplitudes. This method being crucial due to the complexity of the Purcell dynamics[23].

The organization of this article is the following. In section 2, due to space restrictions, we briefly present the concepts and results needed in our study. First of all the model[17] of swimming at low Reynolds number is specialized to the case of a n-links swimmer is standard and leads easily to the dynamical model and the explicit form of the equations[23]. Secondly we recall elements of SR-geometry and introduce the concept of geometric efficiency. Finally the two software (`Bocop` and `HamPath`) and their use in our numerical computations are presented. The section 3 presents the combination of our geometric and numeric analysis to determine optimal strokes of the Copepod swimmer. This case is very important in our study: it is a model of swimmers of an abundant variety of zooplankton which can be observed, it will be used in the future to design a micro-robot to validate our computations. Moreover the model leads to tractable Lie brackets computations, state constraints form a triangle and has a nice geometric interpretation. As a dynamical model it is sufficiently complex to generate a variety of different strokes in accordance with the classification of periodic planar curves[4]. Finally C^1-optimality can be analyzed using the concept of conjugate points and focal point conditions related to periodicity. The concept of geometric efficiency allows to finalize the study. The section 4 is devoted to the three-link Purcell swimmer. The nilpotent approximation is determined to evaluate analytically the strokes with small amplitudes, thanks to integrability. Numeric computations using `Bocop` and `HamPath` software allow to compute more general strokes and to test their optimality with dedicated algorithms to compute conjugate points in the normal and abnormal case. Again, to deal with non unicity of minimizers, in relation with symmetries, we present a solution to the Purcell case.

2. Generalities

2.1. *The mathematical model*

In this section, we present briefly the mathematical models, the complete equations in the case of n-links can being explicitly given[23]. The two swimmers are represented in Fig.1, with the corresponding state variables:

Copepod swimmer: it is formed by gluing together two scallops. Each pair of symmetric links have their length normalized to $l = 1$.
The swimming velocity at x is given by[30]:

$$\dot{x} = \frac{\dot{\theta}_1 \sin(\theta_1) + \dot{\theta}_2 \sin(\theta_2)}{2 + \sin^2(\theta_1) + \sin^2(\theta_2)} \tag{2.1}$$

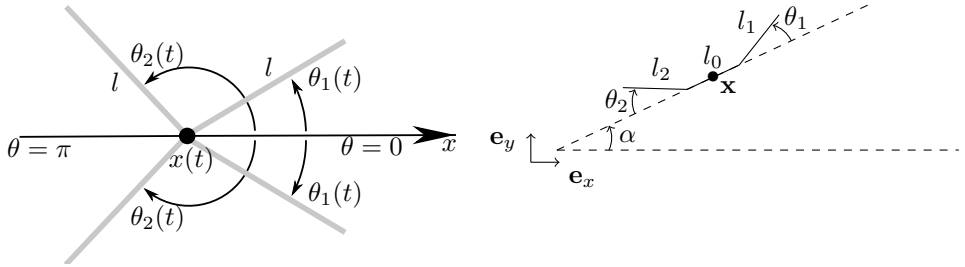

Fig. 1: *(left)* Copepod swimmer, *(right)* Purcell swimmer.

and the controls are the angular velocities

$$\dot\theta_1 = u_1, \quad \dot\theta_2 = u_2.$$

The mechanical power is given by a positive quadratic form $\dot q^\intercal M(q)\dot q$, $q = (x, \theta)$ where

$$M = \begin{pmatrix} 2 - 1/2(\cos^2(\theta_1) + \cos^2(\theta_2)) & -1/2\sin(\theta_1) & -1/2\sin(\theta_2) \\ -1/2\sin(\theta_1) & 1/3 & 0 \\ -1/2\sin(\theta_2) & 0 & 1/3 \end{pmatrix}$$

and using (2.1) this amounts to minimize the quadratic cost:

$$\int_0^T \left(a(q)u_1^2 + 2b(q)u_1u_2 + c(q)u_2^2\right) \mathrm{d}t \tag{2.2}$$

with

$$\begin{aligned} a &= \frac{1}{3} - \frac{\sin^2\theta_1}{2(2 + \sin^2\theta_1 + \sin^2\theta_2)}, \\ b &= -\frac{\sin\theta_1 \sin\theta_2}{2(2 + \sin^2\theta_1 + \sin^2\theta_2)}, \\ c &= \frac{1}{3} - \frac{\sin^2\theta_2}{2(2 + \sin^2\theta_1 + \sin^2\theta_2)}. \end{aligned}$$

Purcell swimmer: this model is much more complex. Denoting $q = (x, y, \alpha, \theta_1, \theta_2)$ it takes the form:

$$\begin{aligned} \begin{pmatrix} \dot x \\ \dot y \\ \dot\alpha \end{pmatrix} &= \frac{1}{\Delta G}\mathcal{R}_\alpha \begin{pmatrix} g_{11} & g_{12} \\ g_{21} & g_{22} \\ g_{31} & g_{32} \end{pmatrix} \begin{pmatrix} \dot\theta_1 \\ \dot\theta_2 \end{pmatrix}, \\ \dot\theta &= u = S(\theta)\tau, \end{aligned} \tag{2.3}$$

where $\mathcal{R}_\alpha$ is the rotation matrix

$$\mathcal{R}_\alpha = \begin{pmatrix} \cos(\alpha) & -\sin(\alpha) & 0 \\ \sin(\alpha) & \cos(\alpha) & 0 \\ 0 & 0 & 1 \end{pmatrix}$$

and $g_{ij}(\theta)$, $\Delta G(\theta)$ and $S(\theta)$ are detailed[23]. Again the cost function u is minimizing the expanded mechanical power

$$\int_0^T \tau \cdot u \, \mathrm{d}t. \tag{2.4}$$

We use the following terminology.

Definition 2.1. The two angular variables $\theta = (\theta_1, \theta_2)$ are called the *shape variables*. A *stroke* of period T consists of a periodic motion in the shape variables.

State constraints. Note that the design of the corresponding system will produce state constraints:

- Copepod case. One has:
$$\theta_1, \theta_2 \in [0, \pi],\ \theta_1 \leq \theta_2.$$
- Purcell case. They depend upon the assumption about the length l_0 of the body and the respective lengths l_1, l_2 of the leg and the arms. We shall perform our computations assuming $l_0 = 2$ and $l_1 = l_2 = 1$. Hence we have the amplitude bounds: $\theta_1, \theta_2 \in [-\pi, \pi]$.

2.2. *Elements of sub-Riemannian geometry*

The optimal control problem is written

$$\dot{q} = \sum_{i=1}^{2} u_i G_i(q), \quad \min_{u(.)} \int_0^T (u^\intercal R(q) u) \, \mathrm{d}t, \tag{2.5}$$

where the set of admissible controls $\mathcal{U}$ is the set of bounded measurable mappings. Note that T can be fixed to 2π. The *length* of a admissible trajectory γ of (2.5) associated with a control u is

$$l(\gamma) = \int_0^T (u^\intercal R(\gamma) u)^{1/2} \, \mathrm{d}t$$

Using the standard concepts of sub-Riemannian geometry[18], we introduce the following.

Definition 2.2. Let D be the distribution $\mathrm{span}\{G_1, G_2\}$. Using a feedback transformation $u = \beta(q)v$, we may choose locally an *orthonormal* frame $F = (F_1, F_2)$ such that the cost function reduces to $v^\intercal v$. Near a point q_0, one can choose the so-called *privileged coordinates* so that the distribution D can be approximated by a *nilpotent distribution* denoted $\widehat{D} = \mathrm{span}\{\widehat{G_1}, \widehat{G_2}\}$. Similarly, one can choose an *nilpotent orthonormal* frame denoted $\{\widehat{F_1}, \widehat{F_2}\}$ to approximate the SR-problem.

Note that this approximation step is particularly important in the Purcell case where the complexity of the model leads to non realizable analytic computations.

2.2.1. *Maximum Principle and computations of geodesic equations*

The Maximum Principle is used to compute the geodesic equations. We write $z = (q, p)$ the symplectic coordinates and $H_F(z) = p \cdot F(q)$ the Hamiltonian lift of the vector field F. Assuming that $\{F_1, F_2\}$ forms an orthonormal frame, the pseudo-Hamiltonian takes the form:

$$H(z, u) = \sum_{i=1}^{2} u_i H_i(z) + \lambda_0 \sum_{i=1}^{2} u_i^2$$

where H_i is the Hamiltonian lift of F_i and λ_0 is a constant which can be normalized to $\lambda_0 = -1/2$ (*normal case*) or $\lambda_0 = 0$ (*abnormal case*). Using the condition: $\frac{\partial H}{\partial u} = 0$ one gets the two cases.

- Normal case: We get $u_i = H_i$ and plugging such u_i into H leads to the true Hamiltonian in the normal case: $H_n = \frac{1}{2}\sum_{i=1}^{2} H_i^2$. The corresponding solutions are called *normal extremals* and their projections on the q-space are called *normal geodesics*.
- Abnormal case: We get the constraints $H_i(z) = 0$, $i = 1, 2$. The corresponding solutions are called *abnormal extremals* and their projections are called *abnormal geodesics*.
- A normal geodesic is called strict if it is not the projection of an abnormal extremal.

This leads to the following concepts.

Definition 2.3. Assuming arc-length parameterization $H_n = 1/2$, the *exponential mapping* is: $\exp_{q_0} : (t, p(0)) \to \Pi(\exp(t\overrightarrow{H_n}(z(0))))$, with $z(0) = (q_0, p(0))$ and Π is the projection: $z \mapsto q$. A *conjugate time* (normal case) is a time t_c such that the function $\exp_{q_0}$ is not of full rank at t_c and the corresponding point is called a *conjugate point* along the geodesic with initial condition $z(0)$. We denote t_{1c} the *first conjugate point*.

2.2.2. *Concepts of SR-geometry adapted to the swimmer problem*

Two aspects of the problem are the state constraints, which will not be theoretically studied in this article, and the boundary conditions related to strokes, which will be introduced next in relation with periodic optimal control. First of all, we recall the necessary optimality conditions[15].

Proposition 2.1. *Let $\bar{q} = (q, q^0)$ and consider the cost extended system denoted $\dot{\bar{q}}(t) = F(\bar{q}(t), u(t))$:*

$$\dot{q} = \sum_{i=1}^{2} u_i G_i(q)$$
$$\dot{q}^0 := L(q, u), \quad q^0(0) = 0$$

and the problem $\min g(\bar{q}(0), \bar{q}(T))$ *for* $u \in U$ *(*U *is the control domain) and with the boundary condition* $(\bar{q}(0), \bar{q}(T)) \in C$ *where* C *is a closed set and* T *is fixed. Introducing* $H(\bar{q}, \bar{p}, u) = \bar{p} \cdot F(\bar{q}, u) = p \cdot \sum_{i=1}^{2} u_i G_i(q) + p_0 L(q, u)$, $\bar{p} = (p, p_0)$, $\lambda \geq 0, (\bar{p}, \lambda) \neq 0$. *Then if* $(\bar{q}^*, u^*)$ *is optimal on* $[0, T]$*, there exists* $\bar{p}^*$ *such that the following necessary conditions are satisfied:*

$$\dot{\bar{q}}^* = \frac{\partial H}{\partial \bar{p}}, \quad \dot{\bar{p}}^* = -\frac{\partial H}{\partial \bar{q}} \qquad a.e.$$
$$H(\bar{q}^*, \bar{p}^*, u^*) = \max_{u \in U} H(\bar{q}^*, \bar{p}^*, u) \qquad a.e\ .$$

Moreover $\max_{u \in U} H$ *is constant and the following transversality conditions hold:*

$$(\bar{p}^*(0), -\bar{p}^*(T)) \in \lambda \nabla_{\bar{q}(0), \bar{q}(T)} g(\bar{q}^*(0), \bar{q}^*(T)) + N_C(\bar{q}^*(0), \bar{q}^*(T)) \tag{2.6}$$

where N_C *is the normal cone.*

Applied to periodic optimal control this lead to the following geometric conditions deduced from the transversality conditions, considering separately periodic conditions and efficiency cost.

Boundary conditions associated with periodicity. We split the state variable q into (q_1, q_2) where q_2 represents the periodic part of q. Let $p = (p_1, p_2)$ be the associated splitting of the adjoint vector. Assuming periodic conditions: $q_2(0) = q_2(T)$ the Maximum Principle leads to the condition:

$$p_2(0) = p_2(T) \tag{2.7}$$

Definition 2.4. A *normal* (resp. *abnormal*) *stroke* is a stroke corresponding to a normal (resp. abnormal) extremal. A *piecewise smooth abnormal stroke* is a piecewise smooth stroke such that each smooth sub-arc corresponds to an abnormal arc.

Shooting equation. To define the *shooting equation*, one restricts the flow to normal extremals, solution of $\overrightarrow{H_n}$, with the following boundary conditions associated with the state variables splitting:

- $q_1(0) = q_{10}, q_1(T) = q_{1T}$ where q_{10}, q_{1T} are fixed,
- $q_2(0) = q_2(T)$, $p_2(0) = p_2(T)$

In the framework of SR-geometry and in relation with the underlying fixed endpoints we have the following two properties[8,1].

Property 2.1. The shooting mapping fails to be locally injective due to the existence of conjugate points.

Property 2.2. The shooting mapping is defined on the cylinder and it fails to be proper due to the existence of abnormal extremals.

Finally in relation with the problem we introduce the following concept.

Definition 2.5. The *geometric efficiency* $\mathcal{E}$ of a stroke γ is defined as

- Copepod swimmer: $\mathcal{E} = x(T)/l(\gamma)$,
- Purcell swimmer: $\mathcal{E} = \sqrt{x(T)^2 + y(T)^2}/l(\gamma)$

that is the ratio between the euclidean displacement along (part of) the state variable and the sub-Riemannian length of the stroke.

In relation with the problem of maximizing the efficiency one introduces the following additional geometric necessary conditions.

Geometric optimality conditions and efficiency. Denoting $\bar{q} = (q, q^0)$ one introduces the cost extended system:

$$\dot{q} = \sum_{i=1}^{2} u_i G_i(q)$$
$$\dot{q}^0 := L(q,u) \quad q^0(0) = 0$$

and maximizing the efficiency leads to $\min g(q(T), q^0(T))$ with $g = -\mathcal{E}$. If $A(\bar{q}(0), T)$ is the accessibility set from $(\bar{q}(0) = q(0), 0)$ at time T anf if $(\bar{q}^*, \bar{p}^*, \bar{u}^*)$ is an optimal solution the geometric optimality conditions are

$$\bar{q}^*(T) \in \partial A(\bar{q}(0), T)$$

and the transversality condition (2.6) gives

$$\bar{p}^*(T) = \lambda \nabla_{\bar{q}} g(\bar{q}^*).$$

2.2.3. *General concepts in SR-Geometry*

Finally we recall the standard concepts of SR-geometry related to the problem with fixed extremities. Having fixed $q(0) = q_0$, the *conjugate locus* $\mathcal{C}(q_0)$ is the set of first conjugate points considering all normal geodesics emanating from q_0. The *cut locus* $C_\Sigma(q_0)$ is the set of points where a (normal or abnormal) geodesic emanating from q_0 ceases to be optimal. The *sphere* $S(q_0, r)$ is formed by the set of points at SR-distance r from q_0.

2.3. `Bocop` *and* `HamPath` *softwares*

- `Bocop` . The so-called *direct* approach transforms an infinite dimensional control problem into a finite dimensional optimization problem. This is done by a discretisation in time applied to the state space, control variables and the dynamics. This method can take into account control and state variables constraints. It is in general less precise than the *indirect* method based on the Maximum Principle, but more robust with respect to the initialization. It will be used to compute optimal strokes satisfying the state constraints

and also as a complementary method to initialize the shooting of the *indirect* method implemented in `HamPath` .

- `HamPath` . This software is based on indirect methods and solve the shooting equation and differential continuation (homotopy) methods and computation of the solutions of the variational equation to check second order conditions of local optimality (conjugate points computations). Having found a stroke using nilpotent approximations and explicit computations (for small amplitudes) or more general solution using `Bocop` , a continuation is performed mainly using as parameter the displacement.

3. The Copepod swimmer

We start recalling two types of strokes[30] employing geometric arguments. These strokes will constitute two important reference cases for our analysis of the Copepod model and which will contribute the motivation of our study.

First case (Fig.2) The two legs are paddling in sequence followed by a recovery stroke performed in unison. In this case, the first step is to steer θ_1 follows by θ_2 from 0 to π, while the unison sequence corresponds to a displacement from π to 0 with the constraint $\theta_1 = \theta_2$. Note it corresponds to a *triangle stroke* and moreover θ_1 and θ_2 stay in the boundary of the domain.

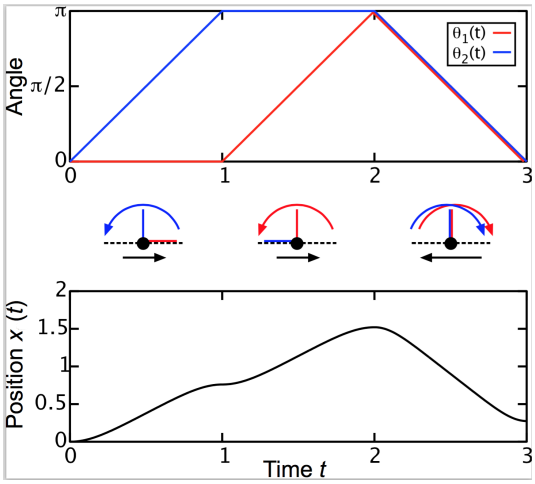

Fig. 2: Two legs paddling in sequence. The legs perform power strokes in sequence and then a recovery stroke in unison, each stroke sweeping an angle π.

Second case (Fig.3) The two legs are assumed to oscillate sinusoidally with period 2π according to

$$\theta_1 = \Phi_1 + a\cos(t), \quad \theta_2 = \Phi_2 + a\cos(t + k_2)$$

with $a = \pi/4$, $\Phi_1 = \pi/4$, $\Phi_2 = 3\pi/4$ and $k_2 = \pi/2$, such parameters being chosen to optimize this efficiency. Assuming $x(0) = 0$, this produces a displacement $x(2\pi) = 0.2$.
Parameters a, Φ_1, Φ_2 and k are designed to maximize the efficiency.

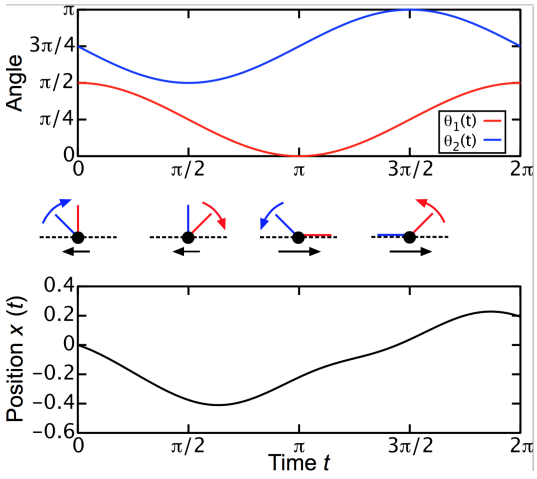

Fig. 3: Two legs oscillating sinusoidally according to $\theta_1 = \pi/4 + a\cos t$ and $\theta_2 = 3\pi/4 + a\cos(t + \pi/2)$, where $a = \pi/4$ is the amplitude. The second leg (blue) oscillates about $\Phi_2 = 3\pi/4$, while the first leg (red) oscillates about $\Phi_1 = \pi/4$ with a phase lag of $\pi/2$. The swimmer position x translates about a fifth of the leg length after one cycle.

3.1. *Abnormal curves in the copepod swimmer*

With $q = (x, \theta_1, \theta_2) \in \mathbb{R}^3$, the dynamics given by the control system

$$\dot{q}(t) = \sum_{i=1}^{2} u_i(t) G_i(q(t)).$$

The Lie bracket of two vectors fields F, G is computed with the convention

$$[F, G](q) = \frac{\partial F}{\partial q}(q)G(q) - \frac{\partial G}{\partial q}(q)F(q).$$

Denoting $p = (p_1, p_2, p_3)$ the adjoint vector associated with q, $z = (q, p)$ and if H_F, H_G are the Hamiltonian lifts $p \cdot F, p \cdot G$, one has:

$$\{H_F, H_G\}(z) = \mathrm{d}H_F(\overrightarrow{H}_G)(z) = p \cdot [F, G](q).$$

Denoting $D = \mathrm{span}\{G_1, G_2\}$, the distribution associated with the control system, one needs to recall basic facts about the classification of such two-dimensional distributions, in relation with abnormal curves[33].

Local classification of two-dimensional distributions in dimension three and abnormal curves. Denoting $H_i(z) = p \cdot G_i(q)$ $i = 1, 2$ the Hamiltonian lifts, abnormal curves are defined by

$$H_1(z) = H_2(z) = 0$$

and differentiating with respect to time and using the dynamics

$$\frac{\mathrm{d}z}{\mathrm{d}t} = \sum_{i=1}^{2} u_i \overrightarrow{H}_i(z)$$

we obtain the relations

$$\{H_1, H_2\}(z) = 0$$
$$u_1 \{\{H_1, H_2\}, H_1\}(z) + u_2 \{\{H_1, H_2\}, H_2\}(z) = 0$$

defining the corresponding abnormal controls. Next, we present only the two stable models related to our study.

Contact case. We say that q_0 is a *contact point* if $\mathrm{span}\{G_1, G_2, [G_1, G_2]\}$ is of dimension 3 at q_0. At a contact point, identified with 0, there exists a system of local coordinates $q = (x, y, z)$ such that

$$D = \ker(\alpha), \qquad \alpha = \mathrm{d}z + (x\mathrm{d}y - y\mathrm{d}x).$$

with the corresponding nilpotent frame

$$\widehat{G_1} = \frac{\partial}{\partial x} + y\frac{\partial}{\partial z}, \widehat{G_2} = \frac{\partial}{\partial y} - x\frac{\partial}{\partial z}$$

Taking $\widehat{G_1}, \widehat{G_2}$ as an orthonormal frame, this leads to the *Heisenberg model* in SR-geometry. Observe that $\mathrm{d}\alpha = -2\,\mathrm{d}y \wedge \mathrm{d}x$ (Darboux form) and that $\frac{\partial}{\partial z}$ is the characteristic direction of $\mathrm{d}\alpha$.

The Martinet case. A point q_0 is a *Martinet point* if at q_0 we have the following property: $[G_1, G_2] \in D = \mathrm{span}\{G_1, G_2\}$ but $\{[[G_1, G_2], G_1], [[G_1, G_2], G_2]\} \not\subseteq D$. Then, there exist local coordinates $q = (x, y, z)$ near q_0 (which can be identified as 0 in these new coordinates) such that

$$D = \ker \omega, \qquad \text{where } \omega := \mathrm{d}z - \frac{y^2}{2}\mathrm{d}x,$$

and the corresponding nilpotent frame takes the form

$$\widehat{G_1} = \frac{\partial}{\partial x} + \frac{y^2}{2}\frac{\partial}{\partial z}, \widehat{G_2} = \frac{\partial}{\partial y}.$$

Moreover, we obtain

$$\widehat{G_3} = [\widehat{G_1}, \widehat{G_2}] = y\frac{\partial}{\partial z}, \ [[\widehat{G_1}, \widehat{G_2}], \widehat{G_1}] = 0, \ [[\widehat{G_1}, \widehat{G_2}], \widehat{G_2}] = \frac{\partial}{\partial z}. \tag{3.1}$$

The surface $\Sigma : y = 0$ where $\widehat{G_1}, \widehat{G_2}, [\widehat{G_1}, \widehat{G_2}]$ are linearly dependent is called the *Martinet surface* and is foliated by abnormal curves, solutions of $\frac{\partial}{\partial x}$. In particular, through the origin it corresponds to the curve $t \to (t, 0, 0)$. Taking $\widehat{G_1}, \widehat{G_2}$ as an orthonormal frame, it corresponds to the so-called *flat Martinet case*.

Computation in the Copepod case. One has

$$G_i = \frac{\sin(\theta_i)}{\Delta}\frac{\partial}{\partial x} + \frac{\partial}{\partial \theta_i},\ i = 1, 2 \ \text{ where } \Delta := 2 + \sin^2(\theta_1) + \sin^2(\theta_2). \tag{3.2}$$

As a consequence we obtain

$$G_3 = [G_1, G_2] = f(\theta_1, \theta_2)\frac{\partial}{\partial x} \quad \text{and} \quad [[G_1, G_2], G_i] = \frac{\partial f}{\partial \theta_i}(\theta_1, \theta_2)\frac{\partial}{\partial x},\ \text{for } i = 1, 2. \tag{3.3}$$

where

$$f(\theta_1, \theta_2) := \frac{2\sin(\theta_1)\sin(\theta_2)(\cos(\theta_1) - \cos(\theta_2))}{\Delta^2}. \tag{3.4}$$

We immediately deduce the following result

Lemma 3.1. *The Martinet surface Σ for the Copepod swimmer is given by the equation $\sin(\theta_1)\sin(\theta_2)(\cos(\theta_1)-\cos(\theta_2)) = 0$. The vector fields G_1, G_2 and $[G_1, G_2]$ are coplanar on Σ, which corresponds to the following values of θ_1 and θ_2:*

- *$\theta_1 = 0$ or π, $\theta_2 = 0$ or π, $\theta_1 = \theta_2$.*

Σ contains the boundary of the physical domain: $\theta_1, \theta_2 \in [0, \pi], \theta_1 \leq \theta_2$, and the edges (with excluded vertices) of the triangle are Martinet points. The associated adjoint vector can be normalized to $p = \left(1, -\frac{-\sin(\theta_1)}{\Delta}, -\frac{-\sin(\theta_2)}{\Delta}\right)$. Thus the triangle is an abnormal stroke.

Remark 3.1. The previous lemma provides the interpretation of the policy represented in Fig.2 which corresponds exactly to the abnormal stroke. Notice that it provides in the $(\theta_1, \theta_2)-$plane the boundary of the physical domain for the Copepod model. A recent contribution[16] proves that such an abnormal curve with corners cannot be optimal (not taking into account a state constraints). Our related analysis with the concept of efficiency will be interesting in the framework of SR-geometry.

3.2. *The normal case*

In the previous section we have discussed the abnormal case, which provide strokes having necessarily a "triangular" shape.

The "Second case" (cf Fig.3) suggests to investigate also strokes which can be described in terms of smooth (trigonometric) functions. This requires dealing with the class of normal extremals. We shall consider both the situations in which we minimize the mechanical energy and the simplified (SR-type) cost where G_1, G_2 are assumed orthonormal. We first provide a feedback transformation which (locally) reduces the mechanical energy to a sum of squares (construction of an orthonormal frame).

3.2.1. *Mechanical energy*

For the SR-problem an orthonormal frame can be established as follows. Using the following feedback transformation

$$\begin{pmatrix} u_1 \\ u_2 \end{pmatrix} = \begin{pmatrix} \cos(\alpha) & \sin(\alpha) \\ -\sin(\alpha) & \cos(\alpha) \end{pmatrix} \begin{pmatrix} v_1 \\ v_2 \end{pmatrix}$$

where $\alpha = \arctan\left(\frac{2\sin(\theta_1)\sin(\theta_2)}{\sin^2(\theta_2)-\sin^2(\theta_1)}\right) = \begin{cases} \arctan\left(\frac{\sin(\theta_1)}{\sin(\theta_2)}\right) & \text{if } \sin(\theta_1) \leq \sin(\theta_2) \\ -\arctan\left(\frac{\sin(\theta_2)}{\sin(\theta_1)}\right) & \text{if } \sin(\theta_1) > \sin(\theta_2) \end{cases}$,
the mechanical energy can be written as

$$\begin{cases} \delta_1 v_1^2 + \delta_2 v_2^2 & \text{if } \sin(\theta_1) \leq \sin(\theta_2) \\ \delta_2 v_1^2 + \delta_1 v_2^2 & \text{if } \sin(\theta_1) > \sin(\theta_2) \end{cases}$$

in which $\delta_1 = \frac{1}{3}$, $\delta_2 = \frac{1}{6}\frac{4-\sin^2(\theta_1)-\sin^2(\theta_2)}{2+\sin^2(\theta_1)+\sin^2(\theta_2)}$.
Introducing

$$\begin{cases} w_1 = \delta_1 v_1,\ w_2 = \delta_2 v_2 & \text{if } \sin(\theta_1) \leq \sin(\theta_2) \\ w_1 = \delta_2 v_1,\ w_2 = \delta_1 v_2 & \text{if } \sin(\theta_1) > \sin(\theta_2) \end{cases}$$

the mechanical energy takes the form $w_1^2 + w_2^2$.

We shall not use this reduction to make our numerical simulations and we use directly the normal Hamiltonian associated with the metric $a(q)u_1^2 + 2b(q)u_1u_2 + c(q)u_2^2$ which is (with $\lambda_0 = -1/2$)

$$H_n(q,p) = \frac{1}{2}\left(a(q)u_1^2 + 2b(q)u_1u_2 + c(q)u_2^2\right), \tag{3.5}$$

where the optimal controls u_1, u_2 are computed according to

$$\begin{cases} H_1(q,p) = a(q)u_1 + b(q)u_2, \\ H_2(q,p) = b(q)u_1 + c(q)u_2 \end{cases}$$

3.2.2. *Simplified cost*

Note that if the cost is simplified to $\int_0^T (u_1^2 + u_2^2)\mathrm{d}t$, some geometric computations can be made, in relation with the Heisenberg case (assuming G_1, G_2 orthonormal) and which can be used in the numerical implementation, in particular to compute strokes with small amplitudes. In this case,

$$H_n = \frac{1}{2}\left(H_1^2 + H_2^2\right)$$

and straightforward computations inside the abnormal triangle are the following using the Poincaré coordinates (q, H), $H = (H_1, H_2, H_3)$ and $H_i = p \cdot G_i(q)$. Indeed:

$$\dot{H}_1 = \mathrm{d}H_1(\vec{H}_n) = \{H_1, H_2\}H_2 = H_2H_3,$$
$$\dot{H}_2 = \mathrm{d}H_2(\vec{H}_n) = \{H_2, H_1\}H_1 = -H_1H_3,$$

Moreover

$$\dot{H}_3 = \mathrm{d}H_3(\vec{H}_n) = \{H_3, H_1\}H_1 + \{H_3, H_2\}H_2,$$

with

$$\{H_3, H_1\}(z) = p \cdot [[G_1, G_2], G_1](q) \text{ and } \{H_3, H_2\}(z) = p \cdot [[G_1, G_2], G_2](q).$$

At a contact point, G_1, G_2, G_3 form a frame, therefore we obtain

$$[[G_1, G_2], G_1](q) = \sum_{i=1}^{3} \lambda_i(q) G_i(q)$$

where $\lambda_1 = \lambda_2 = 0$, $\frac{\partial f}{\partial \theta_1} = \lambda_3 f$.
Similarly,

$$[[G_1, G_2], G_2](q) = \sum_{i=1}^{3} \lambda_i'(q) G_i(q),$$

with

$$\lambda_1' = \lambda_2' = 0, \qquad \frac{\partial f}{\partial \theta_2} = \lambda_3' f.$$

We conclude that

$$\begin{aligned} &\dot{H}_1 = H_2 H_3, \quad \dot{H}_2 = -H_1 H_3, \\ &\dot{H}_3 = H_3 (\lambda_3 H_1 + \lambda_3' H_2). \end{aligned} \tag{3.6}$$

The associated one dimensional distribution can be analyzed setting $\mathrm{d}s = H_3 \mathrm{d}t$ and we obtain

$$\frac{\mathrm{d}H_1}{\mathrm{d}s} = H_2, \qquad \frac{\mathrm{d}H_2}{\mathrm{d}s} = -H_1, \qquad \frac{\mathrm{d}H_3}{\mathrm{d}s} = \lambda_3 H_1 + \lambda_3' H_2. \tag{3.7}$$

In particular, differentiating one more time the first relation of (3.7) with respect to s and using the second relation, we have the harmonic oscillator $H_1'' + H_1 = 0$. Furthermore H_3 can be analyzed using the remaining equation (3.6). Observe that with the approximation λ_3, λ_3' constant, the equation takes the form

$$\frac{\mathrm{d}H_3}{\mathrm{d}s} = A\cos(s + \rho).$$

with A, ρ constant. In those computations, we recognize the Heisenberg case, corresponding to $\lambda_3 = \lambda_3' = 0$.
Observe that when q is not a contact point (that is $G_2 = [G_1, G_2] \in \mathrm{span}\{G_1, G_2\}$, in order to deal with the Martinet case, we can choose the frame G_1', G_2' and G_3', where $G'1 = G_1, G_2' = G_2$ and $G_3' = \frac{\partial}{\partial x}$.

3.2.3. *Numerical results not taking into account the state constraints*

The objective of this section is to investigate the two following problems:

- **Problem 1:** From the micro-local point of view, variety of the different kind of normal strokes e.g. simple loop, eight, limaçon realizable normal strokes by the Copepod swimmer in relation with the classification of planar periodic curves, [4] see Fig.4.

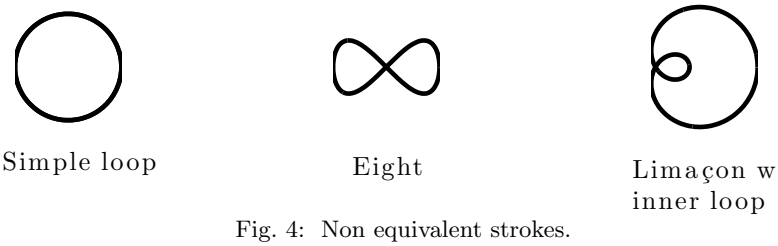

Fig. 4: Non equivalent strokes.

  For this study, we lift the angles $\theta_i \in S^1$ to the covering space $\mathbb{R}$.
- **Problem 2:** Compute the conjugate points along a strict normal stroke to select the candidates for optimality for the fixed endpoints problem.

Numerical methods. The period T is fixed at 2π in our simulations. We use the `HamPath` software[14] at two levels:

(1) The shooting equations associated with the problem are

$$\begin{array}{lll} x(0) = 0, & & x(2\pi) = x_f, \\ \theta_j(0) = \theta_j(2\pi) & j = 1,2, & p_k(0) = p_k(2\pi) \quad k = 2,3. \end{array} \tag{3.8}$$

(2) We consider a normal stroke and we test its optimality by showing the non-existence of conjugate points using the variational equation to compute Jacobi fields. Recall that[8] given a reference curve $(q(t), p(t))$ solution of $\overrightarrow{H_n}$, a time $t_c \in]0, 2\pi]$ is a conjugate time if there exists a Jacobi field $\delta z = (\delta q, \delta p)$, that is a non-zero solution of the variational equation

$$\dot{\delta z}(t) = \frac{\partial \vec{H}_n}{\partial z}(q(t), p(t))\delta z(t) \tag{3.9}$$

such that $\delta q(0) = \delta q(t_c) = 0$. We denote $\delta z_i = (\delta q_i, \delta p_i),\ i = 1...3$, three linearly independent solutions of (3.9) with initial condition $\delta q(0) = 0$. At time t_c we have the following rank condition

$$\text{rank}\{\delta q_1(t_c), \delta q_2(t_c), \delta q_3(t_c)\} < 3. \tag{3.10}$$

Remark 3.2. Note the following result coming from[2,10,32].

Proposition 3.1. *A necessary optimality condition for a strict normal stroke to provide a weak minimizer is the non-existence of a conjugate point on* $]0, 2\pi[$.

Complexity of optimal policies. Fig.5 illustrates four different strokes not taking into account the state constraints confirming the complexity of the model. This can be regarded as examples covering the generic classification of periodic planar curves[4]. Conjugate points are also computed to check the second order optimality conditions. There are no conjugate points on $]0, 2\pi]$ just in the case of the simple loop, but they do appear for the limaçon case, the eight case. Further simulations, taking into account more complicated shapes (combining two "eights") for instance) confirm the presence of conjugate points on $]0, 2\pi[$. *Hence, the only candidates for optimality are the simple loops.*

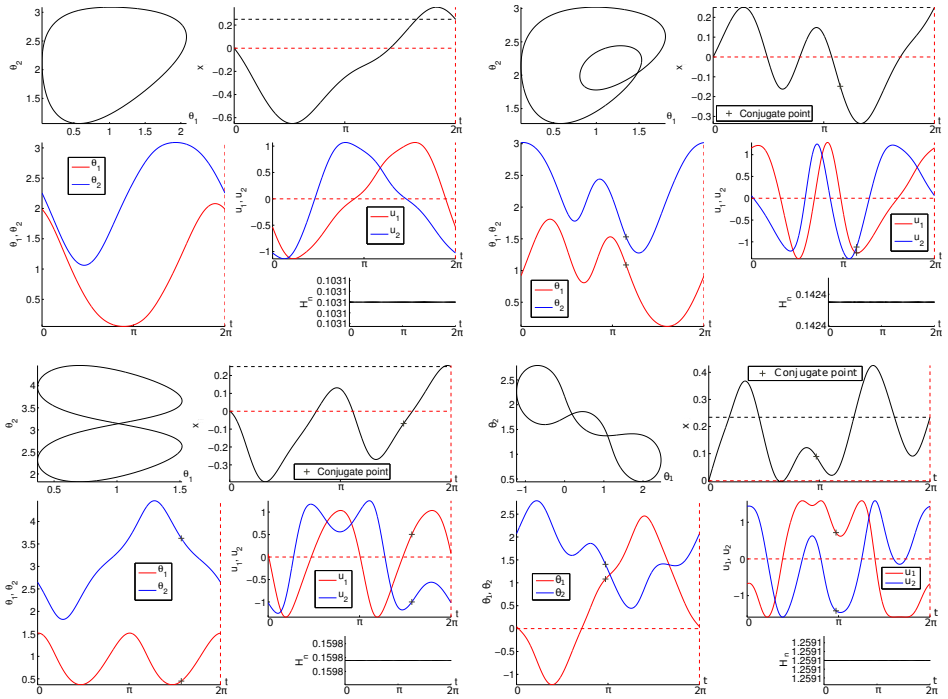

Fig. 5: Normal strokes: simple loop (left), limaçon with inner loop (right) and eight case, and a two self-intersecting case (bottom). First conjugate points on $[0, 2\pi]$ appear with a cross except for the simple loop stroke.

3.2.4. *Optimal curves circumscribed in the triangle of constraints*

We use a combination of the `Bocop` and `HamPath` software.

- `Bocop`: This software is useful when we look for extremals whose state variables have to be confined in a given set, satisfying some state constraints. Fig.6 describes a single loop tangent to the boundary which is used to initialize the shooting algorithm of the `HamPath` software.

- `HamPath`: This software cannot be directly applied to compute the optimal solution using the Maximum Principle with state constraints, due to the complexity of the different principles[10].

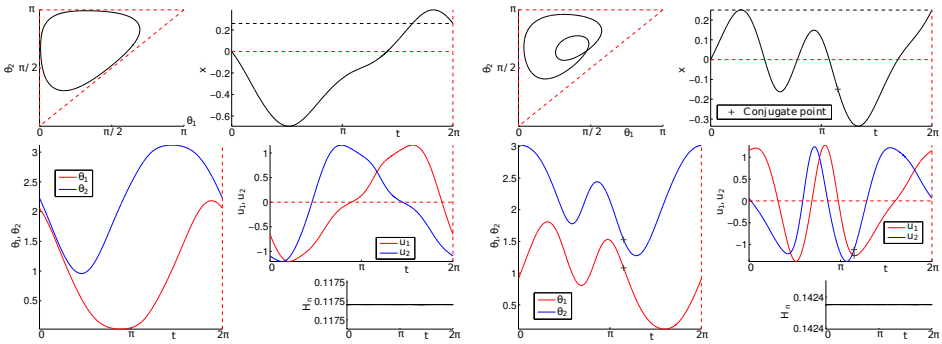

Fig. 6: Normal stroke where the constraints are satisfied: simple loop with no conjugate point on $[0, T]$ (left) and limaçon with inner loop with one conjugate point on $[0, T]$ (right).

Fixing the energy level $H_n = 1/2$, the domain of the exponential map is not compact (it turns out to be a cylinder) and the shooting problem, consisting in finding an initial adjoint vector, is ill-conditioned when we compute normal extremals near the abnormal extremal. Fig.7 highlights this fact by representing the norm of the initial adjoint vector $p = (p_1, p_2, p_3)$ for different displacements, showing that the exponential map is non proper.

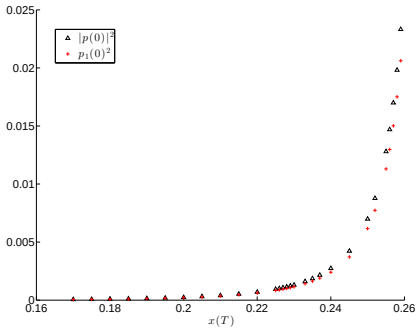

Fig. 7: Norm of the initial adjoint vector $p = (p_1, p_2, p_3)$ and value of $p_1(0)^2$ for normal strokes such that $H_n = 1/2$ and having different displacements, illustrating the non properness of the exponential mapping.

Second order sufficient conditions for the Copepod strokes. The aim of this section is to check second order sufficient conditions for normal extremals represented by simple loop strokes of the Copepod swimmer. We shall employ here particular second order sufficient conditions which can be used in precense of non-uniqueness of minimizers[15]. We provide a short introduction of these results in the Appendix.
We consider the optimal control problem in which we minimize the cost 2.2 over trajectories satisfying

$$\dot{x} = u_1\varphi_1(\theta_1,\theta_2) + u_2\varphi_2(\theta_1,\theta_2), \quad \dot{\theta}_1 = u_1, \quad \dot{\theta}_2 = u_2 \tag{3.11}$$

where $\varphi_i,\ i = 1,2$ are defined in (3.2), such that

$$x(0) = 0, \quad x(T) = x_T, \quad \theta_j(0) = \theta_j(T)\ \ j = 1,2. \tag{3.12}$$

Proposition 3.2. *Take $I = (-\varepsilon,\varepsilon)$ for some $\varepsilon > 0$, and let $(\bar{q}(.), p(.), \bar{u}(.))$ be a normal extremal (on $[0,T]$) where $\bar{q} = (\bar{x},\bar{\theta}_1,\bar{\theta}_2)$, $p = (p_1,p_2,p_3)$ and $\bar{u} = (\bar{u}_1,\bar{u}_2)$. Write $\bar{\theta}_j(.)\ \ j = 1,2, p(.)$ and $\bar{u}(.)$ their corresponding periodic extensions.*
For all $a \in I$ and $t \in [0,T]$, we define

$$\theta_j^a(t) = \bar{\theta}_j(t+a),\ u_j^a(t) = \bar{u}_j(t+a) \quad \text{for } j = 1,2,$$
$$x^a(t) = \int_0^t \left[u_1^a(s)\,\varphi_1(\theta_1^a(s),\theta_2^a(s)) + u_2^a(s)\,\varphi_2(\theta_1^a(s),\theta_2^a(s))\right] \mathrm{d}s$$
$$p^a(t) = (p_1(t), p_2(t+a), p_3(t+a)).$$

Then the normal extremal $(\bar{q}(.), p(.), \bar{u}(.))$ is continuously embedded in the family of extremals $(q^a(.), p^a(.), u^a(.))_{a\in I}$.

In what follows, we denote by $(\bar{q},\bar{u})$ the simple loop of Fig.6 *(left)* with associated adjoint vector p and satisfying (3.12).

Numerical result: *The simple loop $(\bar{q},\bar{u})$ is weak-locally optimal for* (3.11).

(1) To confirm this claim we shall invoke the second order test provided by Thm.Appendix A.2. Conditions (C1)-(C4) and assumptions (H1)-(H4) of Thm.Appendix A.2 are satisfied owing to the data of control system (3.11) and Prop.3.2. Numerical arguments allow to conclude that there is no conjugate point on $[0,T]$ for the normal extremal $(\bar{q}(.), p, \bar{u}(.))$ (see Sec.3.2.3). It implies that the Riccati equations A.2 has a global symmetric solution and the matrix $\phi_{12}(0,T)$ is invertible.
(2) The *Isoda* integrator from the FORTRAN library *odepack* yields the matrix W:

$$W = \begin{pmatrix} 573.04 & -146.59 & -134.55 & -573.04 & 160.65 & 127.23 \\ -146.59 & 37.588 & 34.681 & 146.59 & -41.082 & -32.581 \\ -134.55 & 34.681 & 30.481 & 134.55 & -37.698 & -29.925 \\ -573.04 & 146.59 & 134.55 & 573.04 & -160.65 & -127.23 \\ 160.65 & -41.082 & -37.698 & -160.65 & 46.532 & 34.579 \\ 127.23 & -32.581 & -29.926 & -127.23 & 34.579 & 29.901 \end{pmatrix}.$$

Write

$$m(q_0,q_T)=\begin{pmatrix} x(0)\\ x(T)\\ \theta_1(0)-\theta_1(T)\\ \theta_2(0)-\theta_2(T)\end{pmatrix},\quad \text{hence}\quad \nabla_{q_0,q_T}m(q_0,q_T)=\begin{pmatrix} 1&0&0&0&0&0\\ 0&0&0&1&0&0\\ 0&1&0&0&-1&0\\ 0&0&1&0&0&-1\end{pmatrix}.$$

Consider the linear subspace

$$\mathcal{L}_1=\{\,(y_0,y_T)\in\mathbb{R}^3\times\mathbb{R}^3 \mid \nabla_{q_0,q_T}m(q_0,q_T)\,(y_0\quad y_T)^\intercal=0\,\}.$$

We introduce the matrix M_1 such that $\ker(\nabla_{q_0,q_T}m(q_0,q_T))=\mathrm{Im}(M_1)$. Therefore $M_1^\intercal=\begin{pmatrix}0&0&1&0&0&1\\ 0&1&0&0&1&0\end{pmatrix}$. Standard second order sufficient conditions of Thm.Appendix A.1 lead to check that W is definite-positive on $\mathcal{L}_1$. This is equivalent to check that $\widetilde{W}=M_1^\intercal\,(W^\intercal+W)\,M_1$ is positive-definite. Due to the non-uniqueness of the extremal $(\bar q,p,\bar u)$, $\widetilde{W}$ is not definite-positive (see Table 1).

For the refined second order sufficient conditions of Thm.Appendix A.2, we consider the vector

$$\begin{aligned}\Gamma&=\begin{pmatrix}0&\dot x_2(0)&\dot x_3(0)&0&\dot x_2(0)&\dot x_3(0)\end{pmatrix}^\intercal\\ &=\begin{pmatrix}0&-0.5346&-1.0257&0&-0.5346&-1.0257\end{pmatrix}^\intercal,\end{aligned}$$

the linear subspace

$$\mathcal{L}_2=\mathcal{L}_1\cap\{(y_0,y_T)\in\mathbb{R}^3\times\mathbb{R}^3 \mid \Gamma^\intercal\,(y_0\quad y_T)^\intercal=0\}$$

and the matrix M_2 such that $\ker\begin{pmatrix}\nabla_{q_0,q_T}m(q_0,q_T)\\ \Gamma^\intercal\end{pmatrix}=\mathrm{Im}(M_2)$, hence $M_2^\intercal=\begin{pmatrix}0&-\dot x_3(0)&\dot x_2(0)&0&-\dot x_3(0)&\dot x_2(0)\end{pmatrix}$. Numerical simulations confirm that $\widehat{W}=M_2^\intercal(W^\intercal+W)M_2$ is positive-definite (see Table 1).

We set different absolute and relative tolerances of the integrator to check the zero eigenvalue of $\widetilde{W}$ associated with the vector $\Gamma\in\mathcal{L}_1$ (see Table 1).

Absolute and relative error	(Standard condition) Spec($\widetilde{W}$)	(Refined condition) Spec($\widehat{W}$)
10^{-5}	6.8981×10^{-4} 3.4200	22.553
10^{-10}	-9.1247×10^{-7} 3.4200	22.555

Table 1: The standard condition failed: $\widetilde{W}$ has zero eigenvalue.
The refined condition is satisfied: $\widehat{W}$ is positive-definite.

Comparisons of the geometric efficiency of the strokes. To compare normal and abnormal solutions corresponding to different displacements, in Fig.8 we represent the ratio $\mathcal{E} = x/l$ concerning solutions obtained for a given displacement x and l is the length of the stroke (this quantity does not depend upon the parameterization).

For the triangle, a displacement along the vertical or horizontal edge gives $x = \frac{2\sqrt{3}}{3}\,\mathrm{arctanh}\left(\frac{\sqrt{3}}{3}\right)$ and along the hypotenuse $x = -\sqrt{2}\,\mathrm{arctanh}\left(\frac{\sqrt{2}}{2}\right)$ and the total displacement is $2.742.10^{-1}$.

The length of a normal stroke γ is $l(\gamma) = \int_0^{2\pi} \sqrt{\dot{q}\cdot\dot{q}}\mathrm{d}t$ and is given by $2\pi\sqrt{2H_n}$ where H_n is the energy level. The efficiency curve is displayed in Fig.8 where the normal strokes corresponding to the maximal efficiency is also represented.

Note that the geometric efficiency $\mathcal{E}$ here introduced is different from the concept of efficiency employed in some previous papers[13].

Observe that from computations above obtained for the abnormal stroke, the efficiency turns out to be 5.56×10^{-2}. This result will be compared with the efficiency of normal strokes (cf Fig.8) establishing the optimality of normal strokes (in terms of efficiency).

Conclusions. From our analysis we deduce that the (triangle) abnormal stroke is not optimal. Indeed, one can choose a normal stroke (inside the triangle) such that the displacement is $\bar{x}/2$ with $\bar{x} = 2.742$ and the length is less than $\bar{l}/2$ where $\bar{l}$ is the length of the triangle. Applying twice the normal stroke, we obtain the same displacement $\bar{x}$ than with the abnormal stroke but with a length $< \bar{l}$.

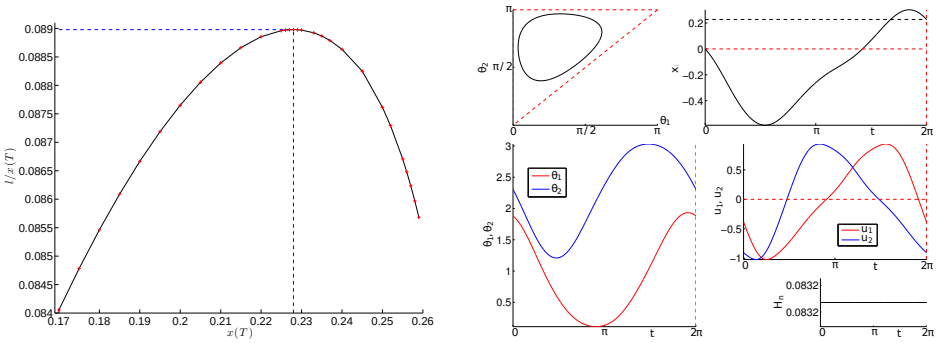

Fig. 8: Efficiency curve (left) and the corresponding minimizing curve with the best performance (right). Note that the efficiency of the abnormal curve is $\mathbf{5.56e^{-2}}$ vs of order $\mathbf{8.89e^{-2}}$ for normal strokes.

4. The Three-Link Purcell swimmer

The controlled dynamics of the Purcell swimmer, briefly recalled in the introduction, is linear with respect to the control[23]

$$\dot{q} = u_1 F_1(q) + u_2 F_2(q) \text{ where } q = (\theta_1, \theta_2, x, y, \alpha) \tag{4.1}$$

where we minimize the mechanical energy given by (2.4).

4.1. *Symmetry properties*

First of all due to the structure of the equations (2.3) we have the following.

Lemma 4.1. *Let* $\bar{q}(t) = (\bar{\theta}_1(t), \bar{\theta}_2(t), \bar{x}(t), \bar{y}(t), \bar{\alpha}(t))$ *and* $q(t) = (\theta_1(t), \theta_2(t), x(t), y(t), \alpha(t))$ *be the solutions associated with* $u(.)$ *with respective initial conditions* $(\theta_{10}, \theta_{20}, 0, 0, 0)$ *and* $(\theta_{10}, \theta_{20}, 0, 0, \alpha_0)$ *then*

$$\begin{aligned} &\bar{\theta}_j(t) = \theta_j(t) \quad j = 1, 2, \quad \alpha(t) = \bar{\alpha}(t) + \alpha_0, \\ &x(t) = \cos(\alpha_0)\bar{x}(t) - \sin(\alpha_0)\bar{y}(t), \\ &y(t) = \sin(\alpha_0)\bar{x}(t) + \cos(\alpha_0)\bar{y}(t). \end{aligned} \tag{4.2}$$

Proof. We denote $A = \begin{pmatrix} 0 & -1 \\ 1 & 0 \end{pmatrix}$, $e^{At} = \begin{pmatrix} \cos(t) & -\sin(t) \\ \sin(t) & \cos(t) \end{pmatrix}$ and using (2.3), one has:

$$\frac{\mathrm{d}}{\mathrm{d}t} \begin{pmatrix} x(t) \\ y(t) \\ \alpha(t) \end{pmatrix} = \begin{pmatrix} \cos(\alpha) & -\sin(\alpha) & 0 \\ \sin(\alpha) & \cos(\alpha) & 0 \\ 0 & 0 & 1 \end{pmatrix} \begin{pmatrix} f_1(t) \\ f_2(t) \\ f_3(t) \end{pmatrix}$$

where $f_i(t)$, $i = 1 \dots 3$ are obtained integrating the θ-dynamics corresponding to $u(.)$ and with $\theta(0) = \theta_0$ and is independent of the (α, x, y)-variables.
One has

$$\alpha(t) = \int_0^t f_3(s)\mathrm{d}s + \alpha_0$$

and denoting $X = (x, y)^\intercal$, $\bar{X} = (\bar{x}, \bar{y})^\intercal$ and $V = (f_1, f_2)^\intercal$,

$$\begin{aligned} \frac{\mathrm{d}X}{\mathrm{d}t} &= e^{A\alpha(t)} V(t) \\ &= e^{A(\alpha_0 + \int_0^t f_3(s)\mathrm{d}s)} V(t) \\ &= e^{A\alpha_0} e^{A\int_0^t f_3(s)\mathrm{d}s} V(t) \\ &= e^{A\alpha_0} \frac{\mathrm{d}\bar{X}}{\mathrm{d}t} \end{aligned}$$

Hence, integrating, one gets the remaining equation (4.2) that is

$$X(t) = e^{A\alpha_0} \bar{X}(t). \qquad \square$$

Lemma 4.2. *Let H_n be the extremal normal Hamiltonian associated with any quadratic cost $\int_0^{2\pi}(a(q)u_1^2+2b(q)u_1u_2+c(q)u_2^2)\mathrm{d}t$. Denoting $(p_\theta,p_x,p_y,p_\alpha)$ the adjoint components, we have the following first integrals*

$$I_1=p_x,\ I_2=p_y,\ I_3=H_n,\ I_4=(p_xy-p_yx)-p_\alpha$$

Proof. The proof results from straightforward computations. □

Corollary 4.1. *Consider the shooting conditions*

- θ,α 2π*-periodic,*
- $x(0)=y(0)=0$,
- $(p_xy-xp_y)(2\pi)=0$
- p_θ,p_α 2π*-periodic,*
- $(x^2+y^2)(2\pi)=r^2$,
- $((p_x,p_y)(2\pi)$ *normal to* $S(r):x^2+y^2=r^2)$.

Since $I_4=(p_xy-xp_y)-p_\alpha$ is a first integral, at $t=0$ and $t=2\pi$ we have $p_xy-p_yx=0$, then we deduce $p_\alpha(0)=p_\alpha(2\pi)$. Hence the assertion p_α is 2π-periodic is equivalent to p is normal to $S(r)$ and one of the conditions can be relaxed and be replaced by $\alpha(0)=0$ to determine the solution.

4.2. *Nilpotent approximation*

Due to the mathematical complexity of the model, the nilpotent approximation will play a crucial role in our analysis. First of all, owing to the integrability of the associated normal extremals in the class of elliptic functions, it will allow to make a micro-local analysis of the different kind of strokes and to estimate the conjugate points using a proper time rescaling. Secondly, the abnormal extremals forming piecewise smooth strokes can be easily computed in this approximation and their optimality studied using the corresponding concept of conjugate point.

4.2.1. *The flat nilpotent model*

There is a unique nilpotent model associated with a 2-dimensional distribution with grow vector $(2,3,5)$ which is described next[12,29].

Definition 4.1. We call the flat Cartan model the 2-dimensional distribution in dimension five defined by the two vector fields:

$$\hat{F}_1(\hat{q})=\frac{\partial}{\partial\hat{q}_1},\ \hat{F}_2(\hat{q})=\frac{\partial}{\partial\hat{q}_2}+\hat{q}_1\frac{\partial}{\partial\hat{q}_3}+\frac{\partial}{\partial\hat{q}_4}+\hat{q}_1^2\frac{\partial}{\partial\hat{q}_5}.$$

where $\hat{q}=(\hat{q}_1,\hat{q}_2,\hat{q}_3,\hat{q}_4,\hat{q}_5)$ will be the privileged coordinates with the following weights: 1 for $\hat{q}_1,\hat{q}_2$, 2 for $\hat{q}_3$ and 3 for $\hat{q}_4,\hat{q}_5$.

4.2.2. *Computations of the nilpotent approximation*

The Purcell system (2.3) can be written as a control system of the form $\dot{q}=Fu=\sum_{i=1}^2u_iF_i$, where the two vectors fields F_1,F_2 have a complicated expression, which can be found in literature[23]. The nilpotent approximation is computed at $q_0=0$

and will provide a nilpotent approximation of the SR-problem for the simplified cost $\int_0^{2\pi}(u_1^2+u_2^2)\mathrm{d}t$ which is sufficient in our theoretical analysis. Assuming that the lengths of the three links are $l_0=2, l_1=l_2=1$, the two-jets of F_1 and F_2 at $q=0$ are

$$\begin{aligned}F_1(q) = &\frac{\partial}{\partial q_1} + \left(-\frac{1}{6}\,q_5 - \frac{4}{27}\,q_1 - \frac{2}{27}\,q_2\right)\frac{\partial}{\partial q_3}\\ &+\left(\frac{1}{6} - \frac{1}{12}\,{q_5}^2 - \frac{2}{27}\,q_5\,q_2 - \frac{4}{27}\,q_5\,q_1 - \frac{1}{27}\,{q_1}^2 - \frac{1}{27}\,q_1q_2 - \frac{1}{36}\,{q_2}^2\right)\frac{\partial}{\partial q_4}\\ &+\left(-\frac{7}{27} + \frac{2}{81}\,{q_1}^2 - \frac{2}{81}\,q_1q_2 - \frac{5}{162}\,{q_2}^2\right)\frac{\partial}{\partial q_5} + O(|q|^3).\end{aligned}$$

$$\begin{aligned}F_2(q) = &\frac{\partial}{\partial q_2} + \left(\frac{1}{6}\,q_5 + \frac{4}{27}\,q_2 + \frac{2}{27}\,q_1\right)\frac{\partial}{\partial q_3}\\ &+\left(-\frac{1}{6} + \frac{1}{12}\,{q_5}^2 + \frac{4}{27}\,q_5\,q_2 + \frac{2}{27}\,q_5\,q_1 + \frac{1}{36}\,{q_1}^2 + \frac{1}{27}\,q_1q_2 + \frac{1}{27}\,{q_2}^2\right)\frac{\partial}{\partial q_4}\\ &+\left(-\frac{7}{27} - \frac{5}{162}\,{q_1}^2 - \frac{2}{81}\,q_1q_2 + \frac{2}{81}\,{q_2}^2\right)\frac{\partial}{\partial q_5} + O(|q|^3)\end{aligned}$$

(In these expressions we are taking the standard normalization $c_t=1, c_n=2c_t$ of the respective tangential and normal drag coefficients[23]).
We compute the local diffeomorphism φ to reduce F_1, F_2 to the nilpotent approximation $\hat{F}_1, \hat{F}_2$ using the sequence $\varphi=\varphi_N\ o\ ...\ o\ \varphi_1 : \mathbb{R}^5\to\mathbb{R}^5$, where $N=13$ and each φ_i is a simple change of coordinates that we describe below.
At each step i, we denote $q=(q_1,q_2,q_3,q_4,q_5)$ the old local coordinates and $Q=(Q_1,Q_2,Q_3,Q_4,Q_5)$ the new ones: $q=\varphi_i(Q)$ and each φ_i has only one non trivial component, the other components being the identity transformation are not specified.

(1) $q_5=\varphi_1^{(5)}(Q_5)=Q_5-\frac{7}{27}Q_1$,
(2) $q_3=\varphi_2^{(3)}(Q_3)=Q_3-\frac{1}{6}Q_5Q_1-\frac{17}{324}Q_1^2-\frac{2}{27}Q_2Q_1$,
(3) $q_4=\varphi_3^{(4)}(Q_4)=Q_4+\frac{1}{6}Q_1-\frac{37}{26244}Q_1^3$,
(4) $q_5=\varphi_4^{(5)}(Q_5)=Q_5+\frac{2}{24}Q_1^3-\frac{2}{162}$,
(5) $q_5=\varphi_5^{(5)}(Q_5)=Q_5-\frac{7}{27}Q_2$,
(6) $q_3=\varphi_6^{(3)}(Q_3)=\frac{5}{81}Q_3+\frac{17}{324}Q_2^2+\frac{1}{6}Q_5Q_2$,
(7) $q_4=\varphi_7^{(4)}(Q_4)=Q_4-Q_3Q_2$,
(8) $q_4=\varphi_8^{(4)}(Q_4)=Q_4+\frac{37}{26244}Q_2^3$,
(9) $q_4=\varphi_9^{(4)}(Q_4)=Q_4-\frac{4482}{8748}Q_5$,
(10) $q_4=\varphi_{10}^{(4)}(Q_4)=Q_4+\frac{2270}{2187}Q_2Q_3+\frac{5}{81}Q_5Q_3+\frac{83}{19683}Q_2^3$,
(11) $q_4=\varphi_{11}^{(4)}(Q_4)=-\frac{83}{2187}Q_4$,
(12) $q_5=\varphi_{12}^{(5)}(Q_5)=Q_5+\frac{1}{27}Q_3Q_2+\frac{2}{243}Q_2^3$,
(13) $q_5=\varphi_{13}^{(5)}(Q_5)=-\frac{1}{54}Q_5-\frac{1}{27}Q_4$.

This leads to a complicated transformation whose role is to relate the privileged coordinates to the physical coordinates $(\theta_1,\theta_2,x,y,\alpha)$ in particular we have:

Lemma 4.3. *The shape variables $\theta = (\theta_1, \theta_2)$ corresponds to the $(\hat{q}_1, \hat{q}_2)$ coordinates.*

4.2.3. *Integration of normal extremal trajectories*

Computing with (4.1), one has

$$\hat{F}_1(\hat{q}) = \frac{\partial}{\partial \hat{q}_1}, \qquad \hat{F}_2(\hat{q}) = \frac{\partial}{\partial \hat{q}_2} + \hat{q}_1 \frac{\partial}{\partial \hat{q}_3} + \hat{q}_3 \frac{\partial}{\partial \hat{q}_4} + \hat{q}_1^2 \frac{\partial}{\partial \hat{q}_5},$$
$$[\hat{F}_1, \hat{F}_2](\hat{q}) = -\frac{\partial}{\partial \hat{q}_3} - 2\hat{q}_1 \frac{\partial}{\partial \hat{q}_5}, \quad [[\hat{F}_1, \hat{F}_2], \hat{F}_1](\hat{q}) = -2\frac{\partial}{\partial \hat{q}_5},$$
$$[[\hat{F}_1, \hat{F}_2], \hat{F}_2](\hat{q}) = \frac{\partial}{\partial \hat{q}_4}.$$

All brackets of length greater than 3 are zero.
Write $\hat{z} = (\hat{q}, \hat{p})$. Introducing the hamiltonian lifts, one has:

$$H_1(\hat{z}) = \hat{p} \cdot \hat{F}_1(\hat{q}) = \hat{p}_1, \qquad H_2(\hat{z}) = \hat{p} \cdot \hat{F}_2(\hat{q}) = \hat{p}_2 + \hat{p}_3\hat{q}_1 + \hat{p}_4\hat{q}_3 + \hat{p}_5\hat{q}_1^2,$$
$$H_3(\hat{z}) = \hat{p} \cdot [\hat{F}_1, \hat{F}_2](\hat{q}) = -\hat{p}_3 - 2\hat{q}_1\hat{p}_5, \quad H_4(\hat{z}) = \hat{p} \cdot [[\hat{F}_1, \hat{F}_2], \hat{F}_1](\hat{q}) = -2\hat{p}_5,$$
$$H_5(\hat{z}) = \hat{p} \cdot [[\hat{F}_1, \hat{F}_2], \hat{F}_2](\hat{q}) = \hat{p}_4.$$

The SR-Cartan flat case is

$$\dot{\hat{q}} = \sum_{i=1}^{2} u_i \hat{F}_i, \quad \min_u \int_0^{2\pi} (u_1^2 + u_2^2) \mathrm{d}t.$$

and the normal Hamiltonian takes the form

$$H_n = \frac{1}{2}(H_1^2 + H_2^2). \tag{4.3}$$

More precisely, using the Poincaré coordinates, the control system is written

$$\begin{aligned} &\dot{\hat{q}}_1 = H_1, \qquad \dot{\hat{q}}_2 = H_2, \qquad \dot{\hat{q}}_3 = H_2\hat{q}_1, \\ &\dot{\hat{q}}_4 = H_2\hat{q}_3, \qquad \dot{\hat{q}}_5 = H_2\hat{q}_1^2. \end{aligned} \tag{4.4}$$

Deriving with respect to the time variable, we have

$$\dot{H}_1 = \mathrm{d}H_1(\vec{H}) = \{H_1, H_2\}H_2 = \hat{p} \cdot [\hat{F}_1, \hat{F}_2](\hat{q})H_2 = H_2H_3,$$
$$\dot{H}_2 = -H_3H_1, \qquad \dot{H}_3 = H_1H_4 + H_2H_5,$$
$$\dot{H}_4 = 0 \quad \text{hence} \quad H_4 = c_4, \quad \dot{H}_5 = 0 \quad \text{hence} \quad H_5 = c_5.$$

Fixing the level energy, $H_1^2 + H_2^2 = 1$ we set $H_1 = \cos(\theta)$ and $H_2 = \sin(\theta)$.

$$\dot{H}_1 = -\sin(\theta)\dot{\theta} = H_2H_3 = \sin(\theta)H_3.$$

Hence $\dot{\theta} = -H_3$ and

$$\ddot{\theta} = -(H_1c_4 + H_2c_5) = -c_4\cos(\theta) - c_5\sin(\theta) = -\omega^2\sin(\theta + \phi)$$

where ω and ϕ are constant. More precisely, we have

$$\omega = \left(\hat{p}_4(0)^2 + 4\hat{p}_5(0)^2\right)^{1/4}, \quad \phi = \arctan\left(\frac{-2\,\hat{p}_5(0)}{\hat{p}_4(0)}\right).$$

Taking $\psi = \theta + \phi$, we get

$$\frac{1}{2}\dot{\psi}^2 - \omega^2\,\cos(\psi) = B, \tag{4.5}$$

where B is the constant

$$B = 1/2\,\left(\hat{p}_3(0) + 2\,\hat{q}_1(0)\hat{p}_5(0)\right)^2 - \hat{p}_1(0)\,\hat{p}_4(0) - 2\,\hat{p}_5(0)\,\hat{p}_2(0) - 2\,\hat{p}_5(0)\,\hat{p}_4(0)\,\hat{x}_3(0).$$

We distinguish the following two cases.

- *Oscillating case.* We introduce $k^2 = \frac{1}{2} + \frac{B}{2\omega^2}$ with $0 < k < 1$ so that (4.5) becomes

  $$\dot{\psi}^2 = 4\omega^2\left(k^2 - \sin^2(\frac{\psi}{2})\right)$$

  and we obtain[19]

  $$\sin(\psi/2) = k\,\mathrm{sn}(u,k), \quad \cos(\psi/2) = \mathrm{dn}(u,k)$$

  where $u = \omega t + \varphi_0$.
  H_1 and H_2 are elliptic functions of the first kind and $\hat{q}_1, \hat{q}_2$, solutions of (4.4), are expressed as

  $$\begin{aligned}\hat{q}_1(u) &= \hat{q}_{10} + \frac{1}{\omega}\Big[-2\,k\,\sin(\phi)\,\mathrm{cn}(u) + (-u + 2\,E(u))\cos(\phi)\Big]\\ \hat{q}_2(u) &= \hat{q}_{20} + \frac{1}{\omega}\Big[-2\,k\,\cos(\phi)\,\mathrm{cn}(u) + (u - 2\,E(u))\sin(\phi)\Big]\end{aligned} \tag{4.6}$$

  where $\hat{q}_{10}$ and $\hat{q}_{20}$ are constant, and $E(.)$ is the elliptic integral of the second kind[19].
- *Rotating case.* We introduce $k^2 = \frac{2\omega^2}{B+\omega^2}$ with $0 < k < 1$ so that (4.5) becomes

  $$\dot{\psi}^2 = \frac{4\omega^2}{k^2}\left(1 - k^2\sin^2(\frac{\psi}{2})\right).$$

  and we obtain[19]

  $$\sin(\psi/2) = \mathrm{sn}(\frac{u}{k},k), \quad \cos(\psi/2) = \mathrm{cn}(\frac{u}{k},k)$$

  where $u = \omega t + \varphi_0$.
  H_1 and H_2 are elliptic functions of the first kind and $\hat{q}_1, \hat{q}_2$ solutions of (4.4) are

expressed as

$$\begin{aligned}\hat{q}_1(u) = \hat{q}_{10} + \frac{1}{\omega}\Bigg[&\Big(1 - \frac{2}{k^2} + 2\,\frac{\mathrm{E}\,(k)}{k^2\,\mathrm{K}\,(k)}\Big)\cos(\phi)\,u \\ &+ \frac{2}{k}\left(\cos(\phi)\,\mathrm{Z}\left(\frac{u}{k}\right) - \sin(\phi)\,\mathrm{dn}\left(\frac{u}{k}\right)\right)\Bigg] \\ \hat{q}_2(u) = \hat{q}_{20} + \frac{1}{\omega}\Bigg[&\Big(\frac{2}{k^2} - 1 - 2\,\frac{\mathrm{E}\,(k)}{k^2\,\mathrm{K}\,(k)}\Big)\sin(\phi)\,u \\ &- \frac{2}{k}\left(\sin(\phi)\,\mathrm{Z}\left(\frac{u}{k}\right) + \cos(\phi)\,\mathrm{dn}\left(\frac{u}{k}\right)\right)\Bigg]\end{aligned} \tag{4.7}$$

where $\hat{q}_{10}$ and $\hat{q}_{20}$ are constant, $K(k), E(k)$ are respectively the complete elliptic integrals of the first and second kind, $Z(.)$ is the Jacobi's Zeta function.

4.2.4. *Computations of strokes with small amplitudes using the nilpotent approximation*

We recall that the physical variables q are related to $\hat{q}$ using the transformation φ. The adjoint variables p are obtained by a Mathieu transformation associated with φ. Strokes with small amplitudes such that $q(0) = 0$ are computed from the nilpotent approximation in the following ways:

- *Oscillating case:*
  The modulus k can be expressed as

$$k(\hat{p}(0)) = \frac{1}{2}\sqrt{\frac{2\sqrt{\hat{p}_4(0)^2 + 4\,\hat{p}_5(0)^2} + \hat{p}_3(0)^2 - 2\,\hat{p}_1(0)\,\hat{p}_4(0) - 4\,\hat{p}_5(0)\,\hat{p}_2(0)}{\sqrt{\hat{p}_4(0)^2 + 4\,\hat{p}_5(0)^2}}} \tag{4.8}$$

  and computing $k(\hat{p}(0))$ such that the linear terms of $\theta_1(t) = \hat{q}_1(\omega t + \varphi_0), \theta_2(t) = \hat{q}_2(\omega t + \varphi_0)$ of (4.6) vanish leads to periodic strokes with eight shapes of period

$$T = \frac{4\,K(k)}{\left(\hat{p}_4(0)^2 + 4\,\hat{p}_5(0)^2\right)^{1/4}}.$$

  The constant $\hat{q}_{10}, \hat{q}_{20}$ are chosen such that $\theta(0) = 0$. The initial adjoint vector $p(0)$ has to check the conditions $H_1(\hat{q}(0), \hat{p}(0))^2 + H_2(\hat{q}(0), \hat{p}(0))^2 = 1$, $k(\hat{p}(0)) \in (0, 1)$ and $\hat{p}_4(0)^2 + 4\,\hat{p}_5(0)^2 \neq 0$. We integrate numerically the stroke in the physical variables starting from $(q(0) = 0, p(0))$ and compute the first conjugate points on $[0, T]$ (see Fig.10).

- *Rotating case:* The modulus k can be expressed as

$$k(\hat{p}(0)) = 2\sqrt{\frac{\sqrt{\hat{p}_4(0)^2 + 4\,\hat{p}_5(0)^2}}{2\,\sqrt{\hat{p}_4(0)^2 + 4\,\hat{p}_5(0)^2} + \hat{p}_3(0)^2 - 2\,\hat{p}_1(0)\,\hat{p}_4(0) - 4\,\hat{p}_5(0)\,\hat{p}_2(0)}} \tag{4.9}$$

  We have $\theta_1(t) = \hat{q}_1(\omega t + \varphi_0), \theta_2(t) = \hat{q}_2(\omega t + \varphi_0)$ where $\hat{q}_1, \hat{q}_2$ are explicitly written in (4.7). We choose $p(0)$ so that $H_1(\hat{q}(0), \hat{p}(0))^2 + H_2(\hat{q}(0), \hat{p}(0))^2 = 1$, $k(\hat{p}(0)) \in (0, 1)$ and such that the denominator of $k(\hat{p}(0))$ is nonzero.
  As $k(\hat{p}(0))$ tends to 0, the linear terms of $\hat{q}_1(u), \hat{q}_2(u)$ of (4.7) tend to 0. This is the case when $\hat{p}_4(0) \to 0$ and $\hat{p}_5(0) \to 0$, and the equation (4.5) becomes

$$\dot{\theta}^2 = \hat{p}_3(0)^2, \tag{4.10}$$

  hence $\ddot{\theta} = 0$ and this case is treated below as the degenerated case.
- *Degenerated case:* We have

$$\ddot{\theta} = 0, \quad \dot{\theta}^2 = \hat{p}_3(0)^2,$$

  hence $\theta(t) = \pm\hat{p}_3(0)\,t + \theta_0$ where θ_0 is a constant and the strokes are given by

$$\hat{q}_1(t) = \hat{q}_{10} + \frac{1}{\pm\hat{p}_3(0)}\sin(\pm\hat{p}_3(0)\,t + \theta_0),\ \hat{q}_2(t) = \hat{q}_{20} - \frac{1}{\pm\hat{p}_3(0)}\cos(\pm\hat{p}_3(0)\,t + \theta_0).$$

Abnormal case. We consider the minimal time problem for the single-input affine system[7]

$$\dot{\hat{q}}(t) = \hat{F}_1(\hat{q}(t)) + u(t)\hat{F}_2(\hat{q}(t))$$

where u is a scalar control.
Denoting $\hat{q}(.)$ a reference minimum time trajectory, since we consider abnormal extremals, it follows from the Pontryagin maximum principle that along the extremal lift of $\hat{q}(.)$, there must hold $H_2(\hat{q}(.), \hat{p}(.)) = 0$ and derivating with respect to t, $\{H_1, H_2\}(\hat{q}(.), \hat{p}(.)) = 0$ must hold too. Thanks to a further derivation, the extremals associated with the controls

$$u_a(\hat{q}, \hat{p}) = \frac{\{H_1, \{H_2, H_1\}\}(\hat{q}, \hat{p})}{\{H_2, \{H_1, H_2\}\}(\hat{q}, \hat{p})} = \frac{2\hat{p}_5}{\hat{p}_4}$$

satisfy the constraints $H_2 = \{H_1, H_2\} = 0$ along $(\hat{q}(.), \hat{p}(.))$ and are solutions of

$$\dot{\hat{q}} = \frac{\partial H_a}{\partial \hat{p}}, \quad \dot{\hat{p}} = -\frac{\partial H_a}{\partial \hat{q}}$$

where H_a is the true Hamiltonian

$$H_a(\hat{q}, \hat{p}) = H_1(\hat{q}, \hat{p}) + u_a H_2(\hat{q}, \hat{p}) = \hat{p}_1 + 2\,\frac{\hat{p}_5\,\left(\hat{p}_2 + \hat{p}_3\,\hat{q}_1 + \hat{p}_4\,\hat{q}_3 + \hat{p}_5\,\hat{q}_1^2\right)}{\hat{p}_4}.$$

From the Pontryagin maximum principle, the constraint $H_1(\hat{q}(.), \hat{p}(.)) = 0$ must hold too. The extremal system subject to the constraints $H_1 = H_2 = \{H_1, H_2\} = 0$

is integrable and solutions can be written as

$$\hat{q}_1(t) = t + \hat{q}_1(0), \qquad \hat{q}_2(t) = 2\,\frac{\hat{p}_5(0)\,t}{\hat{p}_4(0)} + \hat{q}_2(0),$$

$$\hat{q}_3(t) = \frac{\hat{p}_5(0)\,t^2}{\hat{p}_4(0)} + 2\,\frac{\hat{p}_5(0)\,\hat{q}_1(0)\,t}{\hat{p}_4(0)} + \hat{q}_3(0),$$

$$\hat{q}_4(t) = 2/3\,\frac{\hat{p}_5(0)^2 t^3}{\hat{p}_4(0)^2} - 2\,\frac{\hat{p}_5(0)\,\left(\hat{p}_5(0)\,\hat{q}_1(0)^2 + \hat{p}_3(0)\,\hat{q}_1(0) + \hat{p}_2(0)\right)t}{\hat{p}_4(0)^2}$$
$$- \frac{\hat{p}_5(0)\,\hat{p}_3(0)\,t^2}{\hat{p}_4(0)^2} + \hat{q}_4(0),$$

$$\hat{q}_5(t) = 2/3\,\frac{\hat{p}_5(0)\,t^3}{\hat{p}_4(0)} + \frac{(4\,\hat{p}_5(0)\,\hat{q}_1(0) + \hat{p}_3(0))\,t^2}{\hat{p}_4(0)}$$
$$+ 2\,\frac{\left(2\,\hat{p}_5(0)\,\hat{q}_1(0)^2 + \hat{p}_3(0)\,\hat{q}_1(0) + \hat{q}_3(0)\,\hat{p}_4(0) + \hat{p}_2(0)\right)t}{\hat{p}_4(0)} + \hat{q}_5(0),$$

$$\hat{p}_1(t) = \left(-2\,\frac{\hat{p}_5(0)\,\hat{p}_3(0)}{\hat{p}_4(0)} - 4\,\frac{\hat{p}_5(0)^2\hat{q}_1(0)}{\hat{p}_4(0)}\right)t + \hat{p}_1(0),$$

$$\hat{p}_2(t) = \hat{p}_2(0), \qquad \hat{p}_3(t) = -2\,\hat{p}_5(0)\,t + \hat{p}_3(0), \qquad \hat{p}_4(t) = \hat{p}_4(0), \qquad \hat{p}_5(t) = \hat{p}_5(0)$$

with $(\hat{q}_1(0), \hat{q}_2(0), \hat{q}_3(0), \hat{q}_4(0), \hat{q}_5(0), \hat{p}_1(0), \hat{p}_2(0), \hat{p}_3(0), \hat{p}_4(0), \hat{p}_5(0))$ are constant satisfying

$$\hat{p}_1(0) = 0,\ \hat{p}_2(0) = \hat{p}_5(0)\hat{q}_1(0)^2 - \hat{p}_4(0)\hat{q}_3(0),\ \hat{p}_3(0) = -2\hat{p}_5(0)\hat{q}_1(0).$$

Remark 4.1. The θ-projection abnormals are straight lines and will form triangular strokes.

4.3. *Numerical results*

4.3.1. *Computations of conjugate points*

Normal case. In the normal case, we consider the extremal system given by the true Hamiltonian given by (4.3). In section 4.2.3, we described three types of extremals. For each case, we have computed solutions using `HamPath` , representing the control, state and adjoint variables as functions of time (see Fig.9, Fig.10, Fig.11). We also illustrate the conjugate points evaluated according to the algorithm[10], as well as the smallest singular value for the rank test.

Property on the first conjugate point. For the normal extremals in the oscillating case and the rotating case presented in section 4.2.3, we take a large number of random initial adjoint vectors $\hat{p}(0)$ such that $H_1(\hat{q}(0), \hat{p}(0))^2 + H_2(\hat{q}(0), \hat{p}(0))^2 = 1$ and such that $0 < k(\hat{p}(0)) < 1$ where k is given by (4.8) for the oscillating case and by (4.9) for the rotating case. Then we numerically integrate the extremal system.

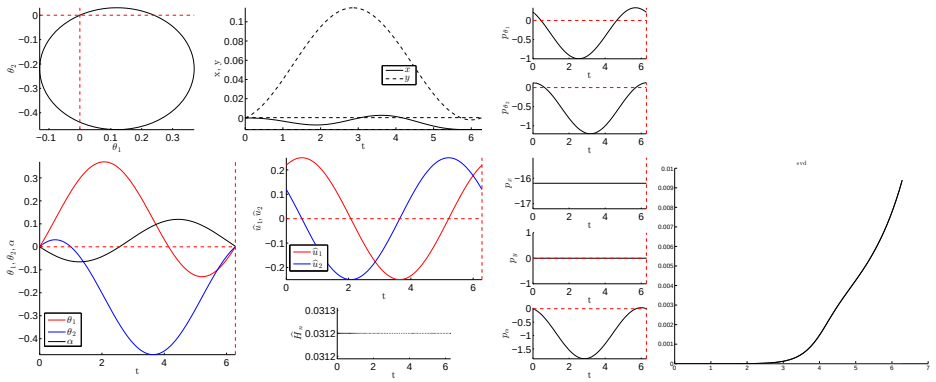

Fig. 9: *(left)* Control, state and adjoint physical variables in the degenerated case of the nilpotent approximation with an simple loop. *(right)* SVD test of conjugate points (no conjugate point on $[0, 2\pi]$).

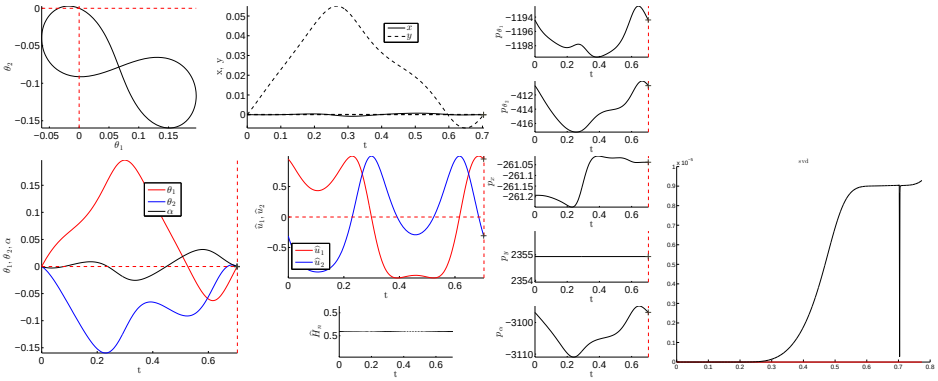

Fig. 10: *(left)* Control, state and adjoint physical variables in the oscillating case of the nilpotent approximation with an eight shape. *(right)* SVD test of conjugate points (the cross stands for the first conjugate point).

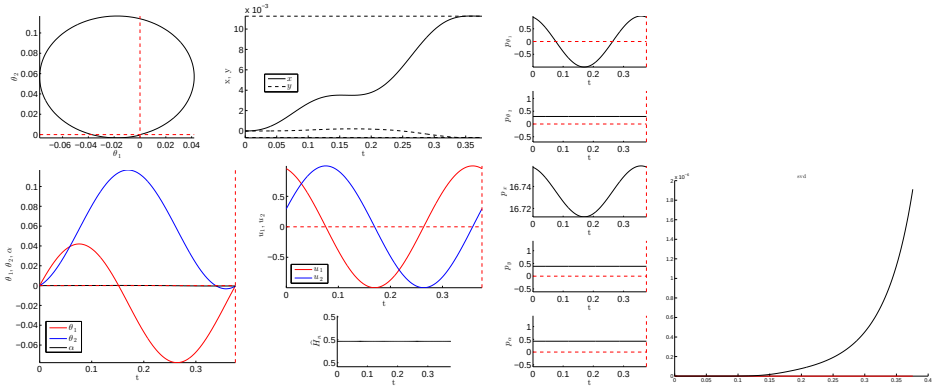

Fig. 11: *(left)* Control, state and adjoint physical variables in the rotating case of the nilpotent approximation ($k = 0.115$). *(right)* SVD test of conjugate points.

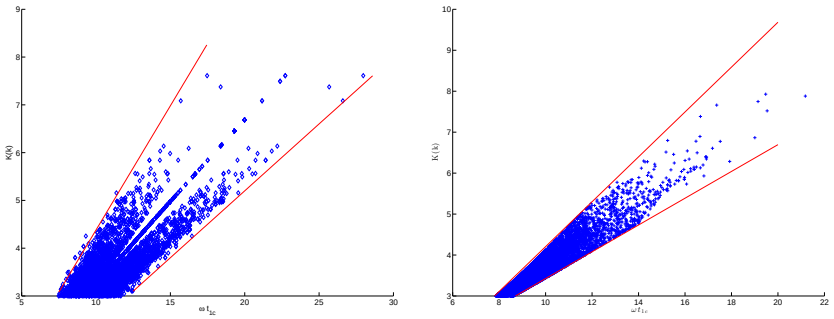

Fig. 12: Conjugate points of normal extremals with constant energy $H_1^2 + H_2^2 = 1$ in the oscillating case *(left)* and in the rotating case *(right)*.

We compute the first conjugate time t_{1c}, the pulsation $\omega = (\hat{p}_4(0)^2 + 4\,\hat{p}_5(0)^2)^{1/4}$, and the complete elliptic integral $K(k)$, where k is the modulus given by (4.8) in the oscillating case or by (4.9) in the rotating case.

Let $\gamma(.)$ be a normal extremal starting at $t = 0$ from the origin and defined on $[0, +\infty[$. As illustrated on Fig.12, there exists a first conjugate point along γ corresponding to a conjugate time t_{1c} satisfying the inequalities:

$$0.34\,\omega\,t_{1c} - 0.4 < K(k) < 0.53\,\omega\,t_{1c} - 0.8 \text{ for the oscillating case,}$$
$$0.33\,\omega\,t_{1c} + 0.16 < K(k) < 0.55\,\omega\,t_{1c} - 1.27 \text{ for the rotating case.}$$

Abnormal case. Fig.13 illustrates the time evolution of the state variables. We check numerically the second order optimality conditions[7]. Both the determinant test and the smallest singular value for the rank condition indicate that there is no conjugate time for abnormal extremals (Fig.14).

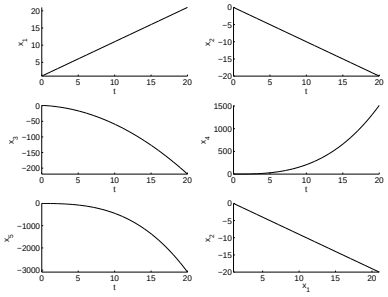

Fig. 13: Abnormal case: state variables for $\hat{q}(0) = (1, 0, 1, 0, 0)$, $\hat{p}(0) = (0, 0, -2, 1, 1)$.

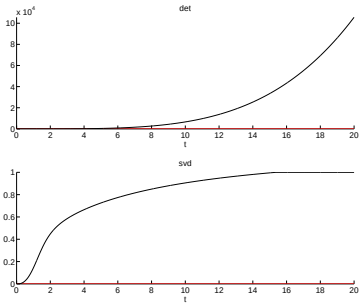

Fig. 14: Abnormal case: the second order sufficient condition indicates there is no conjugate point.

4.3.2. *Computations of optimal strokes using a discrete numerical homotopy*

Method.

- The analytical expressions of $\theta_1(t), \theta_2(t)$, given for the degenerated case and for the oscillating case in section 4.2.3, allow us to compute strokes with small amplitudes of the nilpotent model. Besides, SVD test for conjugate points is also illustrated (see Fig.9 and Fig.10) showing that the simple loop have no conjugate points on $[0, T]$ while the eight stroke have a first conjugate point on $[0, T]$.
- The previous solutions are used to compute strokes for the Purcell swimmer with the $\int_0^T (u_1^2 + u_2^2)\mathrm{d}t$ cost. More precisely, the initial adjoint vector $\hat{p}(0)$ of the nilpotent model gives a good initialization of the shooting algorithm used by `HamPath` to solve the following boundary value problem.

$$\begin{cases} \dot{q} = \frac{\partial \tilde{H}_n}{\partial p}, \quad \dot{p} = -\frac{\partial \tilde{H}_n}{\partial q}, \\ \theta_j(T) = \theta_j(0) \quad j = 1, 2, \\ x(0) = y(0) = \alpha(0) = 0, \\ x(T)^2 + y(T)^2 = c_1,\ \alpha(T) = c_2, \\ p_{\theta_j}(T) = p_{\theta_j}(0) \quad j = 1, 2, p_\alpha(0) = p_\alpha(T) \end{cases} \tag{4.11}$$

where T, c_1, c_2 are fixed constants and $\tilde{H}_n$ is the normal Hamiltonian associated with the $\int_0^T (u_1^2 + u_2^2)\mathrm{d}t$ cost.
Then, with T fixed to 2π and c_2 to 0, we perform a discrete homotopy on the radius c_1 to obtain stroke with larger amplitudes (see Fig.15).

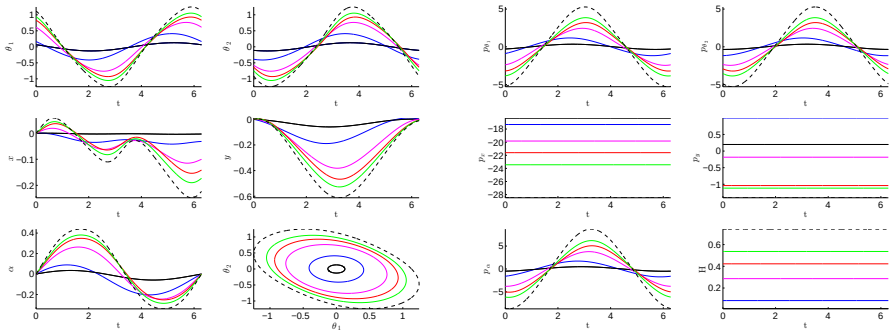

Fig. 15: One parameter family of simple loop strokes of the Purcell swimmer with the $\int_0^T (u_1^2 + u_2^2)\mathrm{d}t$ cost. The continuation is performed on the constant c_1 where we fixed $T = 2\pi$ and $c_2 = 0$.

Fig.16 (resp. Fig.17) illustrates state and adjoint variables for a simple loop stroke (resp. eight stroke) solution of (4.11) and it is obtained from $\hat{p}(0)$ given by the degenerated case (resp. oscillating case). There are no conjugate points

on $[0, 2\pi]$ for the simple loop case, but a conjugate points does appear for the eight case.

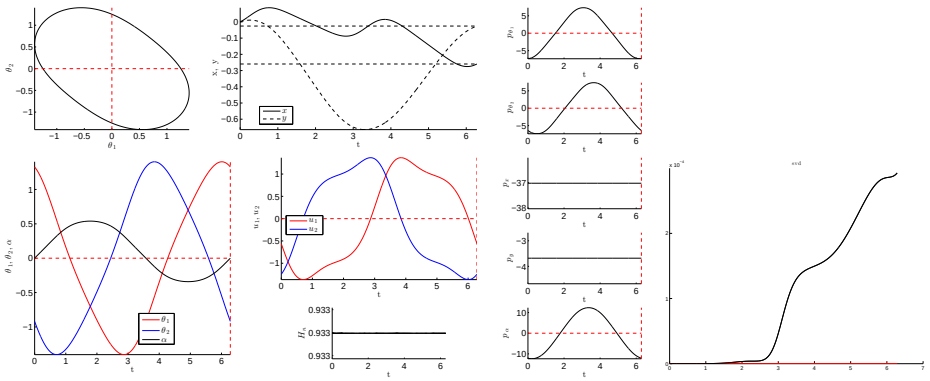

Fig. 16: *(left)* Simple loop stroke for the Purcell swimmer minimizing the cost $\int_0^T (u_1^2 + u_2^2)\mathrm{d}t$, taking $T = 2\pi$, $c_1 = 0.068$, $c_2 = 0$ and imposing the periodicity on α. *(right)* Test of conjugate points (no conjugate point on $[0, 2\pi]$).

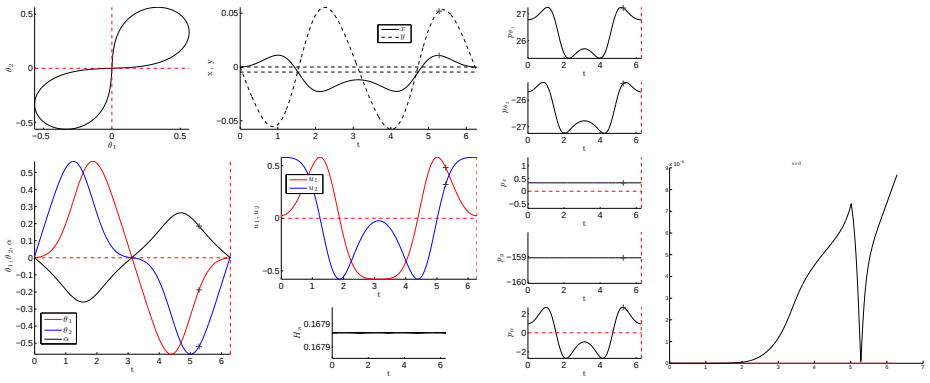

Fig. 17: *(left)* Eight stroke for the Purcell swimmer minimizing the cost $\int_0^T (u_1^2 + u_2^2)\mathrm{d}t$, taking $T = 2\pi$, $c_1 = 4.6e{-}4$, $c_2 = 0$ and imposing the periodicity on α. *(right)* Test of conjugate points (the cross stands for the first conjugate point).

- Let consider the following optimal control problem

$$\begin{cases} \dot{q} = \frac{\partial H_n}{\partial p}, \quad \dot{p} = -\frac{\partial H_n}{\partial q}, \\ \theta_j(T) = \theta_j(0) \quad j = 1, 2, \\ x(0) = y(0) = \alpha(0) = 0, \\ x(T)^2 + y(T)^2 = c_1,\ \alpha(T) = c_2, \\ p_{\theta_j}(T) = p_{\theta_j}(0) \quad j = 1, 2, p_\alpha(0) = p_\alpha(T) \end{cases} \tag{4.12}$$

where $H_n = \frac{1}{2}\left(a(q)u_1^2 + 2b(q)u_1u_2 + c(q)u_2^2\right)$ is the true Hamiltonian associated

with the mechanical cost, and u_1, u_2 are the optimal controls.
We take an extremal of (4.11) to initialize a discrete homotopy with parameter $\lambda \in [0,1]$, of the following optimal control problem

$$\begin{cases} \dot{q} = \frac{\partial H_\lambda}{\partial p}, \quad \dot{p} = -\frac{\partial H_\lambda}{\partial q}, \\ \theta_j(T) = \theta_j(0) \quad j = 1,2, \\ x(0) = y(0) = \alpha(0) = 0, \\ x(T)^2 + y(T)^2 = c_1,\ \alpha(T) = c_2, \\ p_{\theta_j}(T) = p_{\theta_j}(0) \quad j = 1,2, p_\alpha(0) = p_\alpha(T) \end{cases} \tag{4.13}$$

where $H_\lambda = \lambda H_n + (1-\lambda)\tilde{H}_n$. When λ reaches the value 1, we obtain an extremal of (4.12).
Since the latter homotopy is discrete, we may not follow a unique branch and obtain many kind of strokes: Fig.18, Fig.19 and Fig.20 are three different strokes solutions of (4.12) and the SVD rank condition show that the only candidates for optimality are the simple loops.
Then we perform a second homotopy on the radius c_1 to have a one-parameter family of strokes. Fig.21 and Fig.22 are two one-parameter families of solutions of (4.12) corresponding respectively to the strokes of Fig.18 and Fig.19. To compare these two families of strokes, we compute in Fig.23 their geometric efficiencies and we conclude that for a given radius $r = c_1$, the corresponding stroke of the family 1 is more efficient.

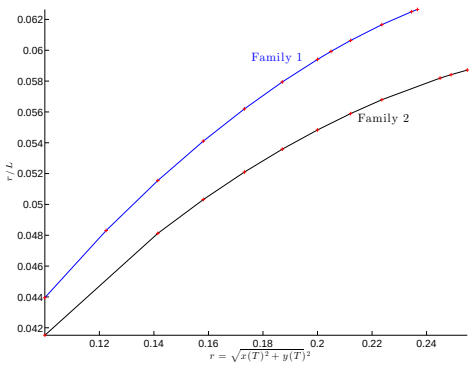

Fig. 23: Comparison of the efficiency between the two families of strokes for the true mechanical cost.

- Result of the continuation: two one-parameter families of simple loop for the mechanical cost appear and their respective efficiency is compared in Fig.23. Note that the efficiency increases with the radius of the circle c_1.

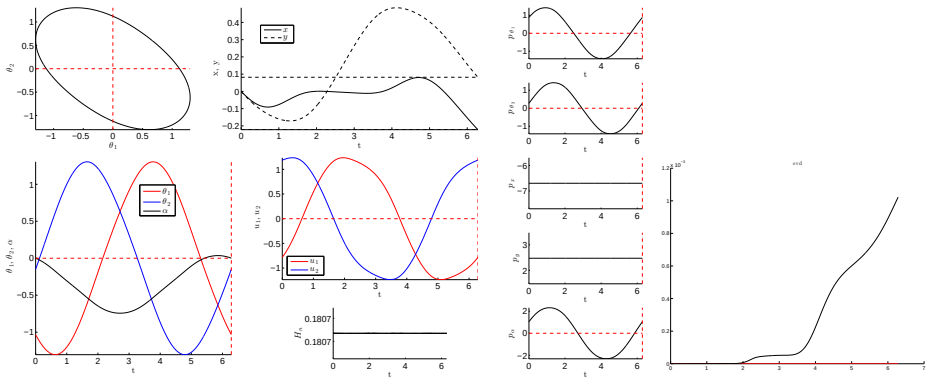

Fig. 18: *(left)* State and adjoint variables for the Purcell swimmer minimizing the mechanical cost, taking $T = 2\pi$, $c_1 = 0.058$ and $c_2 = 0$. *(right)* Test of conjugate points (no conjugate point on $[0, 2\pi]$).

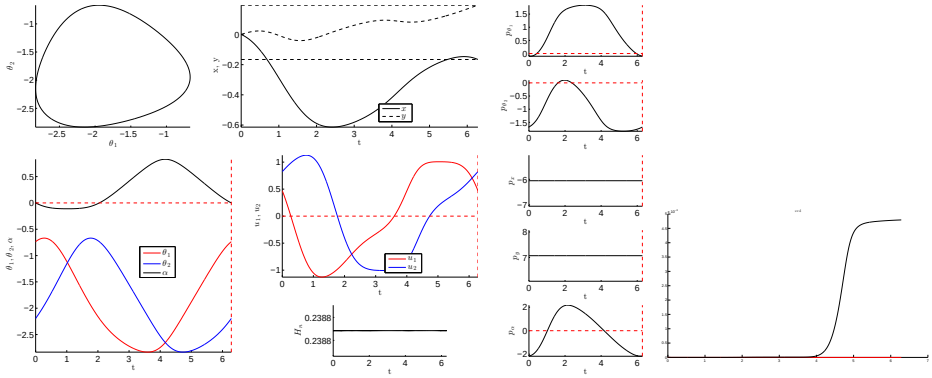

Fig. 19: *(left)* State and adjoint variables for the Purcell swimmer minimizing the mechanical cost, taking $T = 2\pi$, $c_1 = 0.065$ and $c_2 = 0$. *(right)* Test of conjugate points (no conjugate point on $[0, 2\pi]$).

4.4. *Sufficient second order conditions for the Purcell strokes*

The lemma 4.1 gives one symmetry for the Purcell swimmer. We present here an additional symmetry: any time translation of the shape variables (θ_1, θ_2) and the orientation variable α is also a stroke and has the same cost. The presence of these symmetries need particular second order sufficient conditions[15] (see the Appendix for a brief summary). For this purpose, we provide numerical results on second order sufficient conditions for normal extremals of the Purcell swimmer.

We consider the optimal control problem in which we minimize the cost 2.4 over

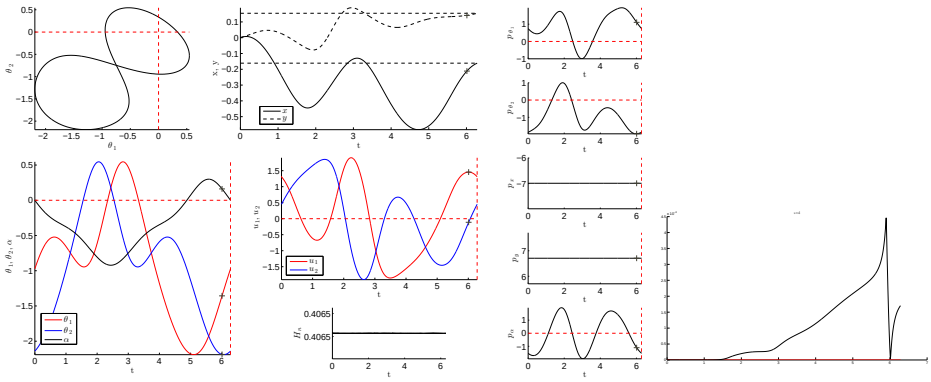

Fig. 20: *(left)* State and adjoint variables for the Purcell swimmer minimizing the mechanical cost, taking $T = 2\pi$, $c_1 = 0.05$ and $c_2 = 0$. *(right)* Test of conjugate points (the cross stands for the first conjugate point).

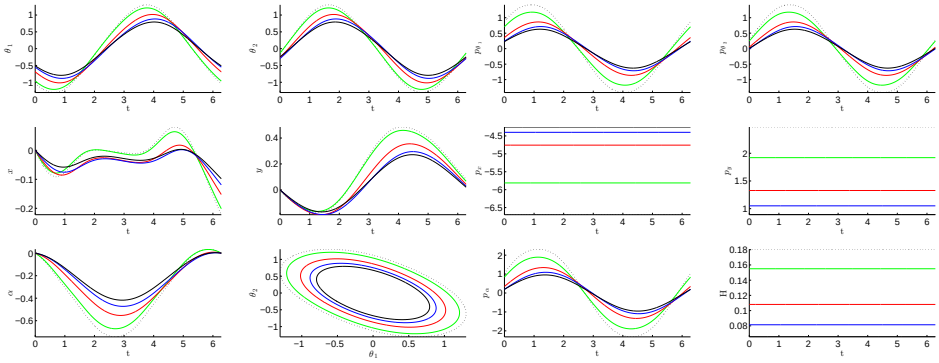

Fig. 21: Family 1 of strokes for the Purcell swimmer minimizing the mechanical cost. We fixed $T = 2\pi$ and $c_2 = 0$ and the family of strokes is obtained by a continuation on c_1.

trajectories satisfying

$$\begin{aligned} &\dot\theta_j = u_1 F_{1j}(q) + u_2 F_{2j}(q) \quad j = 1, 2, \\ &\dot x = u_1 F_{13}(q) + u_2 F_{23}(q), \quad \dot y = u_1 F_{14}(q) + u_2 F_{24}(q), \\ &\dot\alpha = u_1 F_{15}(q) + u_2 F_{25}(q). \end{aligned} \tag{4.14}$$

where F_{1k}, F_{2k} $k = 1 \cdots 5$ are the k^{th} component of F_1, F_2 mentionned in (4.1), such that

$$\begin{aligned} &\theta_j(0) = \theta_j(T) \quad j = 1, 2, \quad \alpha(0) = \alpha(T), \\ &x(0) = 0,\ y(0) = 0,\ x(T)^2 + y(T)^2 = r \text{ (r is fixed)} . \end{aligned} \tag{4.15}$$

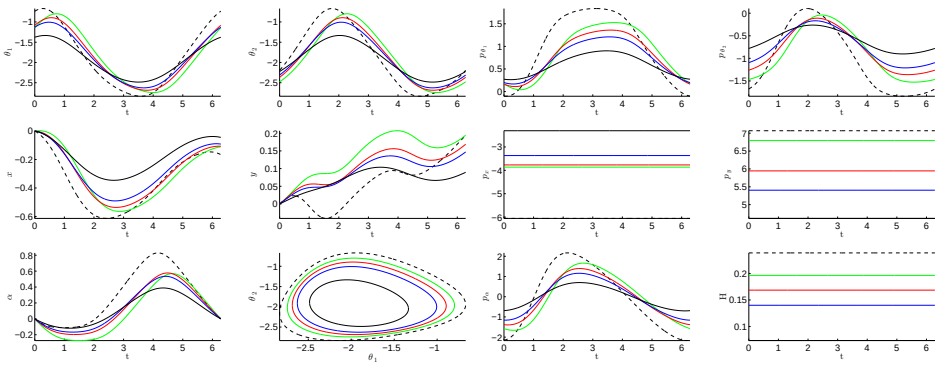

Fig. 22: Family 2 of strokes for the Purcell swimmer minimizing the mechanical cost. We fixed $T = 2\pi$ and $c_2 = 0$ and the family of strokes is obtained by a continuation on c_1.

Proposition 4.1. *Take* $a = (\phi, \sigma) \in I = (-\varepsilon, \varepsilon)^2$ *for some* $\varepsilon > 0$. *Let* $\bar{q} = (\bar{\theta}_1, \bar{\theta}_2, \bar{x}, \bar{y}, \bar{\alpha})$ *solution of* (4.14)-(4.15) *associated with control* $\bar{u} = (\bar{u}_1, \bar{u}_2)$ *and adjoint vector* p. *For all* $a \in I$ *and* $t \in [0, T]$, *we define*

$$\begin{aligned} &u_j^a(t) = \bar{u}_j(t+\sigma),\ \theta_j^a(t) = \bar{\theta}_j(t+\sigma) \quad j = 1, 2, \\ &x^a(t) = \cos(\phi)x^\sigma(t) + \sin(\phi)y^\sigma(t), \\ &y^a(t) = \sin(\phi)x^\sigma(t) - \cos(\phi)y^\sigma(t), \\ &\alpha^a(t) = \bar{\alpha}(t+\sigma) + \phi \end{aligned} \tag{4.16}$$

where

$$x^\sigma(t) = \int_0^t \Big(u_1^a(s)F_{13}(\theta_1^a(s), \theta_2^a(s), \bar{\alpha}(s+\sigma)) + u_2^a(s)F_{23}(\theta_1^a(s), \theta_2^a(s), \bar{\alpha}(s+\sigma))\Big)\mathrm{d}s,$$

$$y^\sigma(t) = \int_0^t \Big(u_1^a(s)F_{14}(\theta_1^a(s), \theta_2^a(s), \bar{\alpha}(s+\sigma)) + u_2^a(s)F_{24}(\theta_1^a(s), \theta_2^a(s), \bar{\alpha}(s+\sigma))\Big)\mathrm{d}s.$$

Then the normal extremal $(\bar{q}(.), p(.), \bar{u}(.))$ *is continuously embedded in the family of extremals* $(q^a(.), p^a(.), u^a(.))_{a\in I}$ *where* $p^a(.)$ *is the adjoint vector associated with* $q^a(.), u^a(.))$.

We apply the algorithm[15] to the simple loop of Fig.19 satisfying (4.14)-(4.15) with associated adjoint vector p and we have the following result.

Numerical result: *The simple loop* $(\bar{q}, \bar{u})$ *is weak-locally optimal for* (3.11).

(1) Due to (4.14) and Prop.4.1, the Purcell model verifies the conditions (C1)-(C4) and assumptions (H1)-(H4) required by Thm.Appendix A.2.
The Riccati equations A.2 has a global symmetric solution and the matrix $\phi_{12}(0, T)$ is invertible owing to the fact that there is no conjugate points for the normal extremal $(\bar{q}(.), p, \bar{u}(.))$.

(2) The *Isoda* integrator from the FORTRAN library *odepack* yields the matrix:

$$W = \begin{pmatrix} 36.7491 & -12.3797 & -90.3501 & -38.4486 & 45.9572 & -20.9543 & 12.3334 & 90.3501 & 38.4486 & -22.0849 \\ -12.3797 & 12.7351 & 63.8598 & -2.19107 & -4.48021 & 5.29771 & -14.0060 & -63.8598 & 2.19107 & -7.52291 \\ -90.3501 & 63.8598 & 356.119 & 72.4282 & -72.3005 & 50.6364 & -65.6286 & -356.119 & -72.4282 & 5.46840 \\ -38.4486 & -2.19107 & 72.4283 & 155.119 & -58.0160 & 27.2663 & -1.54193 & -72.4283 & -155.119 & 30.3765 \\ 45.9572 & -4.48021 & -72.3005 & -58.0160 & 74.6500 & -29.6527 & 3.10041 & 72.3005 & 58.0160 & -51.0282 \\ -20.9543 & 5.29771 & 50.6364 & 27.2663 & -29.6527 & 11.6627 & -5.47480 & -50.6364 & -27.2663 & 15.3254 \\ 12.3334 & -14.0060 & -65.6286 & -1.54192 & 3.10041 & -5.47479 & 15.7573 & 65.6286 & 1.54192 & 9.86428 \\ 90.3501 & -63.8598 & -356.119 & -72.4282 & 72.3005 & -50.6364 & 65.6286 & 283.095 & 72.4282 & -5.46840 \\ 38.4486 & 2.19107 & -72.4283 & -155.119 & 58.0160 & -27.2663 & 1.54193 & 72.4283 & 82.0946 & -30.3765 \\ -22.0850 & -7.52291 & 5.46840 & 30.3766 & -51.0282 & 15.3254 & 9.86428 & -5.46840 & -30.3766 & 44.9320 \end{pmatrix}.$$

We set

$$\mathcal{L}_1 = \{\, (y_0, y_T) \in \mathbb{R}^5 \times \mathbb{R}^5 \mid \nabla_{q_0,q_T} m(q_0, q_T)\, (y_0 \quad y_T)^\intercal = 0 \,\}.$$

where

$$m(q_0, q_T) = \begin{pmatrix} \theta_1(0) - \theta_1(T) \\ \theta_2(0) - \theta_2(T) \\ x(0) \\ y(0) \\ \alpha(0) - \alpha(T) \\ x(T)^2 + y(T)^2 - r \end{pmatrix}.$$

We take the matrix N_1 such that $\ker(\nabla_{q_0,q_T} m(q_0, q_T)) = \mathrm{Im}(N_1)$.
Now from the symmetry of Prop.4.1, we define

$$\Gamma_\phi = \begin{pmatrix} \nabla_\phi q^a(0) \\ \nabla_\phi q^a(T) \end{pmatrix}_{\phi=0},\ \Gamma_\sigma = \begin{pmatrix} \nabla_\sigma q^a(0) \\ \nabla_\sigma q^a(T) \end{pmatrix}_{\sigma=0} \text{ and } \widehat{\Gamma} = (\Gamma_\phi \quad \Gamma_\sigma). \tag{4.17}$$

We consider the linear subspaces

$$\begin{aligned} \mathcal{L}_\phi &= \mathcal{L}_1 \cap \{(y_0, y_T) \in \mathbb{R}^5 \times \mathbb{R}^5 \mid \Gamma_\phi^\intercal\, (y_0 \quad y_T)^\intercal = 0\}, \\ \mathcal{L}_\sigma &= \mathcal{L}_1 \cap \{(y_0, y_T) \in \mathbb{R}^5 \times \mathbb{R}^5 \mid \Gamma_\sigma^\intercal\, (y_0 \quad y_T)^\intercal = 0\}, \\ \widehat{\mathcal{L}} &= \mathcal{L}_1 \cap \{(y_0, y_T) \in \mathbb{R}^5 \times \mathbb{R}^5 \mid \widehat{\Gamma}^\intercal\, (y_0 \quad y_T)^\intercal = 0\} \end{aligned}$$

and the matrices N_ϕ, N_σ and $\widehat{N}$ such that

$$\mathcal{L}_\phi = \mathrm{Im}(N_\phi), \quad \mathcal{L}_\sigma = \mathrm{Im}(N_\sigma), \quad \widehat{\mathcal{L}} = \mathrm{Im}(\widehat{N}).$$

We take two different tolerances for the integrator used to obtain the matrix W from the Hamiltonian system (A.3). Table 2 shows that the matrices $\widetilde{W}_1 = N_1^\intercal\, (W^\intercal + W)\, N_1$, $\widetilde{W}_\phi = N_\phi^\intercal\, (W^\intercal + W)\, N_\phi$ and $\widetilde{W}_\sigma = N_\sigma^\intercal\, (W^\intercal + W)\, N_\sigma$ have zero eigenvalues (whose eigenvectors are Γ_ϕ and Γ_σ). In particular, $\widetilde{W}_1$ is not definite-positive then the standard sufficient second order conditions fail.
Also, the refined second order sufficient conditions of Thm.Appendix A.2 are satisfied since the eigenvalues of $\widehat{W} = \widehat{N}^\intercal\, (W^\intercal + W)\, \widehat{N}$ are positive.

Absolute and relative error	(Standard condition) Spec($\widetilde{W}_1$)	Spec($\widetilde{W}_\phi$)	Spec($\widetilde{W}_\sigma$)	(Refined condition) Spec($\widehat{W}$)
10^{-4}	1319.91 3.44629 -2.61575×10^{-5} -4.17860×10^{-3}	35380.1 3.46392 -4.18945×10^{-3}	1366.83 -4.10573×10^{-4} 14.5123	36179.7 13.8018
10^{-7}	1320.17 3.44676 9.81190×10^{-6} -5.40128×10^{-6}	35386.9 3.46438 -4.84724×10^{-6}	1367.10 9.85195×10^{-6} 14.5151	36186.9 13.8037

Table 2: The standard condition failed: $\widetilde{W}_1$ has zero eigenvalues.
The refined condition is satisfied: $\widehat{W}$ is positive-definite.

5. Conclusion

For further studies the program is the following.

- Nilpotent approximations are not sufficient in the Copepod case where only simple loops can be obtained and for the Purcell swimmer and moreover they are not a generic model to study the SR-balls. A more complete program is to compute higher order approximations for the contact case[1] and for the Martinet case[8] to generate generic strokes. Also it will clarify the distribution of conjugate points, crucial for the convergence of continuation methods.
- The numerical results have to be completed to compute strokes with larger amplitudes for the Purcell case and the analysis pursued to deal with different links parameters.
- A more complete analysis in relation with non smooth abnormal minimizers has to be done in order to clarify the optimality status of abnormal strokes, taking into account the state constraints and with respect to C^0-optimality.

Appendix A. Sufficient conditions for non-unique minimizers

We summarize here a second order 'alternative test' which gives sufficient conditions for non-unique minimizers,[15]. We consider the optimal control problems with end-point constraints of the form

$$\begin{cases} \text{Minimize } J(q(.),u(.)) = \int_0^T L(q(t),u(t))\mathrm{d}t \\ \text{subject to} \\ \dot{x}(t) \;=\; F(q(t),u(t)) \quad \text{a.e. } t \in [0,T]\,, \\ u(t) \;\in\; U \quad \text{a.e. } t \in [0,T]\,, \\ c(q(0),q(T)) = 0\,, \end{cases} \tag{A.1}$$

in which $F(.,.) : \mathbb{R}^n \times \mathbb{R}^m \to \mathbb{R}^n$ and $L(.,.) : \mathbb{R}^n \times \mathbb{R}^m \to \mathbb{R}$ are given functions of class $\mathcal{C}^2$ with continuous second derivatives w.r.t. (q,u) variables, $c(.,.) : \mathbb{R}^n \times \mathbb{R}^n \to \mathbb{R}^\ell$ is a given function of class $\mathcal{C}^2$ with continuous second derivatives w.r.t. (q_0, q_T)

variables, and $U \subset \mathbb{R}^m$ is a given set. We say that $((\bar{q}(.), \bar{u}(.))$ is a (local) *weak* minimizer if there exists $\delta > 0$ such that

$$J((\bar{q}(.), \bar{u}(.)) \leq J((q(.), u(.)))$$

for any trajectory/control couple $(q(.), u(.))$ which is admissible for the control system of (A.1) such that $\|\bar{q}(.) - q(.)\|_{L^\infty} \leq \delta$ and $\|\bar{u}(.) - u(.)\|_{L^\infty} \leq \delta$. Take a reference weak normal extremal $(\bar{q}(.), \bar{u}(.), p(.), \nu)$ which means that the vector-valued function $p(.) \in W^{1,1}([0,T]; \mathbb{R}^n)$, the vector $\nu \in \mathbb{R}^\ell$ together with the trajectory/control couple $(\bar{q}(.), \bar{u}(.))$ satisfy the following conditions

(i) $-\dot{p}(t) \;=\; p^T(t)\, \frac{\partial F}{\partial q}(\bar{q}(t), \bar{u}(t)) \;-\; \frac{1}{2}\, \frac{\partial L}{\partial q}(\bar{q}(t), \bar{u}(t))$ a.e.

(ii) $p(t) \cdot F(\bar{q}(t), \bar{u}(t)) - \frac{1}{2} L(\bar{q}(t), \bar{u}(t)) = \max\limits_{u \in U} \{\, p(t) \cdot F(\bar{q}(t), u) - \frac{1}{2} L(\bar{q}(t), u) \,\}$ a.e.

(iii) $[-p^T(0),\ p^T(T)] = \nu^T D_{q_0, q_T} c(\bar{q}(0), \bar{q}(T))$.

We say that $(\bar{q}(.), \bar{u}(.), p(.), \nu)$ is continuously embedded in a family of weak normal extremals

$$\{(x^\alpha(.), u^\alpha(.), p^\alpha(.), \nu^\alpha) \mid \alpha \in \mathcal{A}\}$$

where $\mathcal{A}$ is an open ball centered at the origin in some Euclidean space, such that $(\bar{q}(.), \bar{u}(.), p(.), \nu) = (q^0(.), u^0(.), p^0(.), \nu^0)$, and the following properties are satisfied:

(C1): for each $\alpha \in \mathcal{A}$, $(q^\alpha(.), u^\alpha(.), p^\alpha(.), \nu^\alpha)$, is a weak normal extremal such that:

$$J((q^\alpha(.), u^\alpha(.))) = J((\bar{q}(.), \bar{u}(.))) \qquad \text{and} \qquad c(q^\alpha(0), q^\alpha(T)) = c(\bar{q}(0), \bar{q}(T)) = 0\,,$$

(C2): the map $\alpha \to (q^\alpha(.), u^\alpha(.), p^\alpha(.), \nu^\alpha) \;:\; \mathcal{A} \to L^\infty \times L^\infty \times L^\infty \times \mathbb{R}^\ell$ is strongly continuous,

(C3): the map $\alpha \to (q^\alpha(0), q^\alpha(T)) \;:\; \mathcal{A} \to \mathbb{R}^n \times \mathbb{R}^n$, is of class $\mathcal{C}^1$,

(C4): the following $(d+k) \times 2n$ matrix has full row rank:

$$\begin{pmatrix} \Gamma^T \\ D_{q_0, q_T} c((\bar{q}(0), \bar{q}(T))) \end{pmatrix}$$

where

$$\Gamma := \left[\begin{matrix} D_\alpha q^\alpha(0) \\ D_\alpha q^\alpha(T) \end{matrix} \right] \Bigg|_{\alpha = 0}\,.$$

Consider the Riccati system:

$$\begin{cases} \dot{P} + PA + A^T P + Q - (B^T P + D^T)^T R^{-1} (B^T P + D^T) = 0 \\ P^T(.) \;=\; P(.)\,, \end{cases} \tag{A.2}$$

where

$$A(t) := \frac{\partial F}{\partial q}(\bar{q}(t), \bar{u}(t)), \quad B(t) := \frac{\partial F}{\partial u}(\bar{q}(t), \bar{u}(t))$$

and

$$\begin{pmatrix} Q(t) & D(t) \\ D^T(t) & R(t) \end{pmatrix} := \begin{pmatrix} \frac{\partial^2 \mathcal{H}}{\partial q^2}(\bar{q}(t), p(t), \bar{u}(t)) & \frac{\partial^2 \mathcal{H}}{\partial q u}(\bar{q}(t), p(t), \bar{u}(t)) \\ \frac{\partial^2 \mathcal{H}}{\partial q u}^T(\bar{q}(t), p(t), \bar{u}(t)) & \frac{\partial^2 \mathcal{H}}{\partial u^2}(\bar{q}(t), p(t), \bar{u}(t)) \end{pmatrix} .$$

Consider the transition matrix associated with the linearized Hamiltonian system

$$\begin{cases} \frac{\mathrm{d}}{\mathrm{d}s}\Phi(t,s) = Z\Phi(t,s) \\ \Phi(s,s) = \mathrm{Id} \ , \end{cases} \tag{A.3}$$

where

$$Z := \begin{bmatrix} A - BR^{-1}D^T & -BR^{-1}B^T \\ -Q + DR^{-1}D^T & -AR^{-1}B^T \end{bmatrix}$$

Set

$$\Phi(0,T) =: \begin{bmatrix} \phi_{11} & \phi_{12} \\ \phi_{21} & \phi_{22} \end{bmatrix}$$

and

$$W := \begin{bmatrix} \phi_{22}\phi_{12}^{-1} & \phi_{21} - \phi_{22}\phi_{12}^{-1}\phi_{11} \\ -\phi_{12} & \phi_{12}^{-1}\phi_{11} \end{bmatrix} .$$

We shall also assume

(H1): the functions F, L, c are of class $\mathcal{C}^2$ with continuous second derivatives w.r.t. all variables,
(H2): there exists $\rho > 0$ such that $R(t) > \rho \mathrm{I}$, for all $t \in [0,T]$,
(H3): $(A(.), B(.))$ ia controllable on $[0,T]$,
(H4): $\bar{u}(.)$ is essentially bounded.

Theorem Appendix A.1 (Standard conditions, 15). *Take a weak normal extremal for $(q(.), u(.))$. Assume hypotheses (H1)-(H4) are satisfied. Suppose that*

(i): the Riccati equation (A.2) has a symmetric solution on $[0,T]$,
(ii): there exists $\gamma > 0$ such that

$$\begin{bmatrix} \xi_0^T & \xi_1^T \end{bmatrix} W \begin{bmatrix} \xi_0 \\ \xi_1 \end{bmatrix} > \gamma \left| \begin{bmatrix} \xi_0 \\ \xi_1 \end{bmatrix} \right|^2 ,$$

for all vectors $\xi_0, \xi_1 \in \mathbb{R}^n \setminus \{0\}$ satisfying $D_{q_0} c((\bar{q}(0), \bar{q}(T)))\xi_0 + D_{q_T} c((\bar{q}(0), \bar{q}(T)))\xi_1 = 0$.
Then $(\bar{q}(.), \bar{u}(.))$ is a weak locally unique minimizer.

The sufficient second order conditions of the previous theorem are well-known and we stress here that such conditions provide that the weak local minimizer is actually unique.

Theorem Appendix A.2 (Refined conditions, 15). *Assume that hypotheses (H1)-(H4) are satisfied. Suppose that a weak normal extremal $(\bar{q}(.), \bar{u}(.), p(.), \nu)$ can be continuously embedded in a family of weak normal extremals, and that*

(i): the Riccati equation (A.2) has a symmetric solution on $[0,T]$,
(ii): there exists $\gamma > 0$ *such that*

$$\begin{bmatrix}\xi_0^T & \xi_1^T\end{bmatrix} W \begin{bmatrix}\xi_0 \\ \xi_1\end{bmatrix} > \gamma \left|\left|\begin{bmatrix}\xi_0 \\ \xi_1\end{bmatrix}\right|\right|^2 ,$$

for all vectors $\xi_0, \xi_1 \in \mathbb{R}^n \setminus \{0\}$ *satisfying*

$$D_{q_0} c((\bar{q}(0),\bar{q}(T)))\xi_0 + D_{q_T} c((\bar{q}(0),\bar{q}(T)))\xi_1 = 0 \qquad \textit{and} \qquad \Gamma^T \begin{bmatrix}\xi_0 \\ \xi_1\end{bmatrix} = 0 \ .$$

Then $(\bar{q}(.),\bar{u}(.))$ *is a weak local minimizer.*

Acknowledgment

J. Rouot is supported by the French Space Agency CNES, R&T action R-S13/BS-005-012 and by the région Provence-Alpes-Côte d'Azur,

References

1. A.A. Agrachev, El-H.C. Alaoui, J.-P. Gauthier, I. Kupka, Generic singularities of sub-Riemannian metrics on $\mathbb{R}^3$, *C. R. Acad. Sci. Paris Sér. I Math.* **322** 4 (1996) 377–384.
2. A.A. Agrachev, A.V. Sarychev, Strong minimality of abnormal geodesics for 2-distributions, *J. Dynam. Control Systems* **1** 2 (1995) 139–176.
3. A. Bellaïche, The tangent space in sub-Riemannian geometry, *J. Math. Sci. (New York)* n.4 **83** (1997) 461–476.
4. M. Berger, La taxonomie des courbes. Pour la science, **297** (2002) 56–63.
5. P. Bettiol, P., Bonnard, B., Giraldi, L., Martinon, P., Rouot, J., The three links Purcell swimmer and some geometric problems related to periodic optimal controls. Rad. Ser. Comp. App. **18**, Variational Methods, Ed. by M. Bergounioux et al. (2016).
6. F. Bonnans, D. Giorgi, S. Maindrault, P. Martinon, V. Grélard, *Bocop - A collection of examples, Inria Research Report, Project-Team Commands*, **8053** (2014).
7. B. Bonnard, J.-B. Caillau, E. Trélat, Second order optimality conditions in the smooth case and applications in optimal control, *ESAIM Control Optim. Calc. Var.* **13** (2007) 207–236.
8. B. Bonnard, M. Chyba, Singular trajectories and their role in control theory, Mathématiques & Applications **40**, Springer-Verlag, Berlin (2003).
9. B. Bonnard, M. Claeys, O. Cots, P. Martinon, Geometric and numerical methods in the contrast imaging problem in nuclear magnetic resonance. *Acta Appl. Math.* **135** (2015) 5–45.
10. B. Bonnard, L. Faubourg, E. Trélat, Mécanique céleste et contrôle des véhicules spatiaux. Mathématiques & Applications, Springer-Verlag **51** Berlin (2006).
11. B. Bonnard, E. Trélat, On the role of abnormal minimizers in sub-Riemannian geometry, *Ann. Fac. Sci. Toulouse Math. (6)* n. 3 **10** (2001) 405–491.
12. E. Cartan, Les systèmes de Pfaff a cinq variables et les équations aux derivées partielles du second ordre, *Ann. Sci. École Normale* **27** (1910) 109–192.
13. T. Chambrion, L. Giraldi, A. Munnier, Optimal Strokes for Driftless Swimmers: A General Geometric Approach, *Submitted* (2014).
14. O. Cots, *Contrôle optimal géométrique : méthodes homotopiques et applications*, Phd thesis, Institut Mathématiques de Bourgogne, Dijon, France (2012).

15. C. Gavriel, R.B. Vinter, Second order sufficient conditions for optimal control problems with non-unique minimizers: an abstract framework, *Appl. Math. Optim.* **70** (2014) 411–442.
16. E. Hakavuori, E. Le Donne, Non-minimality of corners in sub-Riemannian geometry. Preprint (2015).
17. J. Happel, H. Brenner, Low Reynolds number hydrodynamics with special applications to particulate media. *Prentice-Hall, Inc., Englewood Cliffs, N.J.* (1965).
18. F. Jean, Control of Nonholonomic Systems: from Sub-Riemannian Geometry to Motion Planning, Springer International Publishing, SpringerBriefs in Mathematics (2014).
19. D.F. Lawden, Elliptic functions and applications, *Applied Mathematical Sciences*, Springer-Verlag, New York **80** (1989).
20. M. J. Lighthill, Note on the swimming of slender fish, *J. Fluid Mech.* **9** (1960) 305–317.
21. J. Lohéac, J-F. Scheid, M. Tucsnak, Controllability and time optimal control for low Reynolds numbers swimmers, *Acta Appl. Math.* **123** (2013) 175–200.
22. R. Montgomery, A tour of subriemannian geometries, their geodesics and applications. American Mathematical Society, Providence, RI. **91** (2002).
23. E. Passov, Y. Or, Supplementary notes to: Dynamics of Purcells three-link microswimmer with a passive elastic tail, *EPJ E* **35** (2012) 1–9.
24. H. Poincaré, Mémoire sur les courbes définies par une équation différentiable, *Jour. Math. Pures et Appl.* **7** 3 (1881) 375-422; **8** (1882) 251-296; **1** 4 (1885) 167-244; **2** (1886) 151-217.
25. H. Poincaré, Œuvres. Tome VII, *Éditions Jacques Gabay, Sceaux* (1996).
26. L.S. Pontryagin, V.G. Boltyanskii, R.V. Gamkrelidze and E.F. Mishchenko, The mathematical theory of optimal processes, *Interscience Publishers John Wiley & Sons, Inc.* New York-London (1962).
27. E.M. Purcell, Life at low Reynolds number, *Am. J. Phys.* **45** (1977) 3–11.
28. L. Rifford, Singulière minimisante en géométrie sous-Riemannienne, *Séminaire Bourbaki*, 68ème année, 1113 (2016), à paraître.
29. Yu.L. Sachkov, Symmetries of flat rank two distributions and sub-Riemannian structures, *Trans. Amer. Math. Soc.* n.2 **356** (2004) 457–494.
30. D. Takagi, Swimming with stiff legs at low Reynolds number, *Phys. Rev. E 92.* (2015).
31. R.B. Vinter, Optimal control, *Systems & Control: Foundations & Applications* (2000) xviii–507.
32. Q. Wang and J.L. Speyer, Necessary and sufficient conditions for local optimality of a periodic process, *SIAM J. Control Optim.* n.2 **28** (1990) 482–497.
33. M. Zhitomirskiĭ, Typical singularities of differential 1-forms and Pfaffian equations, *American Mathematical Society, Providence, RI.* **113** (1992).